Deep mitochondrial DNA phylogeographic divergence in the threatened aoudad *Ammotragus lervia* (Bovidae, Caprini)

Authors: Louiza Derouiche[a*], Ahmed Irzagh[b], Rafiq Rahmouni[c], Redouane Tahri[d], Mohamed Hadjeloum[e], Rachid Bouhadad[a], Carlos Fernandes[f*]

'Accepted manuscript' version of the article published in the journal *Gene*, DOI: 10.1016/j.gene.2020.144510,
https://www.sciencedirect.com/science/article/abs/pii/S0378111920301797

Affiliations: [a]LBEIG, Population Genetics & Conservation Unit, Faculté des Sciences Biologiques, Université des Sciences et de la Technologie Houari Boumediene, BP 32 El-Alia, Bab Ezzouar, 16111 Algiers, Algeria; [b]Département de Biotechnologie, Faculté des Sciences de la Nature et de la Vie, Université Saad Dahlab de Blida, route de Soumâa, BP 270, 09000 Blida, Algeria; [c]Réserve de Chasse de Tlemcen, Direction Générale des Forêts (DGF), Boulevard de Lala Sitti, Tlemcen, Algeria; [d]'Nature Algérie', Béchar, Algeria; [e]Bureau de la Gestion et Protection de la Faune, Direction Générale des Forêts (DGF), Algiers, Algeria; [f]CE3C – Centre for Ecology, Evolution and Environmental Changes, Faculdade de Ciências, Universidade de Lisboa, 1749-016 Lisboa, Portugal

[*]**Corresponding authors**
E-mail: derouiche_fatma@yahoo.fr; cafernandes@fc.ul.pt

Abstract

The aoudad or Barbary sheep (*Ammotragus lervia*) is a threatened ungulate emblematic of North Africa, whose population structure and subspecific taxonomy have not been examined genetically. This knowledge is essential and urgently needed to inform ongoing conservation and management efforts. We analysed the mitochondrial cytochrome *b* gene and four nuclear genes (casein kappa, spectrin beta nonerythrocytic 1, thyroglobulin, thyrotropin subunit beta) for the first phylogeographic survey of the aoudad, and uncovered a deep Mediterranean-Saharan mitochondrial split separating two highly distinct evolutionary lineages. Their level of divergence is greater than or comparable to those observed between several pairs of congeneric species of different caprine genera. The split was estimated to have occurred in the Early Pleistocene, about 1.3 million years ago. None of the four nuclear genes surveyed, chosen because they have been used in phylogeographic and species-level phylogenetic studies of bovids, allowed us to detect, likely due to their slow evolutionary rate, the substantial and geographically coherent subdivision revealed by mitochondrial DNA. This study is evidence and testament to the ability of mitochondrial DNA, probably unrivalled by any other single-locus marker, as an exploratory tool for investigating population genealogy and history and identifying potential evolutionarily significant units for conservation in animals.

Keywords: Barbary sheep, phylogeography, divergence times, molecular systematics, subspecies, caprine

Highlights:

- The aoudad or Barbary sheep (*Ammotragus lervia*) is a threatened ungulate emblematic of North Africa
- First molecular study of phylogeography and intraspecific systematics in the aoudad
- Deep Mediterranean-Saharan mitochondrial split separating two highly distinct clades
- New insights on the evolutionary history, subspecific taxonomy and conservation units in the aoudad

1. Introduction

The aoudad or Barbary sheep *Ammotragus lervia* (Pallas, 1777) is a medium-sized wild ungulate belonging to a monotypic genus in the tribe Caprini of the family Bovidae (Kingdon, 1982; Kingdon, 1997; Hassanin and Douzery, 1999; Kingdon and Hoffmann, 2013). The species was formerly widespread in rugged and mountainous terrain from arid and semiarid regions to open forests in North Africa, but their range and population size have decreased dramatically due to hunting, poaching, habitat destruction, and competition with domestic livestock (Loggers et al., 1992; Kingdon, 1997; Shackleton, 1997). It has become extinct or endangered in many parts of its former distribution area (Cuzin, 1996; Manlius et al., 2003; Mimoun et al., 2017), so much so that it is considered a top conservation priority among caprines (Shackleton, 1997) and is currently listed as 'Vulnerable' in the IUCN Red List of Threatened Species (Cassinello et al., 2008). Unlike the situation in its indigenous range, the aoudad has been successfully introduced for hunting into Spain (southeast mainland and island of La Palma in the Canary archipelago) and southwestern United States, where it has become invasive and a threat to local biodiversity (Gray and Simpson, 1980; Cassinello et al., 2004; Nogales et al., 2006; Acevedo et al., 2007).

Given the severe population decline and fragmentation across its native North African distribution (Shackleton, 1997), there is an urgent need to determine the species' population genetic structure to inform the conservation and management of the aoudad. Based on pelage colour and patterns, shape and curvature of the horns, and geographical distribution, six subspecies are recognized (Rothschild, 1913, 1921; Allen, 1939; Gray and Simpson, 1980; Grubb,

2005; Cassinello et al., 2008) as follows: *A. l. lervia* (Atlas Aoudad; occurring in northern Morocco, northern Algeria, and northern Tunisia), *A. l. sahariensis* (Saharan Aoudad; distributed in Mauritania, southern Morocco, the Adrar des Iforas in Mali, south Algeria, southwestern Libya, and the Tibesti Mountains in northwestern Chad), *A. l. fassini* (Libyan Aoudad; present in extreme southern Tunisia and in Libya), *A. l. angusi* (Aïr Aoudad; found in the Aïr and Termit mountains of Niger), *A. l. blainei* (Kordofan Aoudad; in Sudan, where currently it is probably restricted to the Red Sea hills, and it may also be the subspecies inhabiting the Ennedi Mountains in northeast Chad), and *A. l. ornata* (Egyptian Aoudad; in both the Eastern and Western Deserts of Egypt) (Fig. S1). However, the taxonomy of the aoudad is unclear because the morphological distinctiveness of the subspecies is uncertain and the consistency of the morphological differences has not been thoroughly evaluated (Cassinello et al., 2008). Moreover, there is debate regarding the exact geographic ranges of the described subspecies (Kingdon, 1997; Shackleton, 1997; Cassinello, 1998). Therefore, it is necessary to evaluate the validity of the subspecies and determine the geographical limits of the valid ones. Genetic studies using mitochondrial DNA (mtDNA) sequence data have proven useful in such contexts (e.g. Rambau et al., 2003; Mulcahy, 2008; Andersen and Light, 2012; Prieto-Torres et al., 2018). The fact is that the aoudad has been understudied genetically, particularly in terms of the geographic distribution of its genetic diversity in its native range. The bulk of previous molecular research has sought to clarify the phylogenetic relationships of the aoudad with other Caprini (Curtain and Fudenberg, 1973; Manwell and Ann Baker, 1975, 1977; Hight and Nadler, 1976; Ludwig and Fischer, 1998; Mereu et al., 2008; Pirastru et al., 2009). Recent studies do not indicate a close

affinity with either sheep (*Ovis* spp.) or goats (*Capra* spp.), but instead with the Arabian tahr (*Arabitragus jayakari*) and the chamois (*Rupicapra* spp.) (Hassanin et al., 2009; Peng et al., 2012; Jiang et al., 2013; Yang et al., 2013).

In Algeria, the largest country in Africa, the abundance and distribution of the aoudad in the north of the country have decreased significantly in the last decades, and the northern boundaries of natural populations generally coincide with the Saharan Atlas and the southern slopes of the Aurès Mountains (Kowalski and Rzebik-Kowalska, 1991; De Smet, 1997; Bounaceur et al., 2016). In response to this, and to promote the conservation and recovery of the species in northern Algeria, aoudads have been reintroduced into two protected areas: the Moutas hunting reserve, near Tlemcen in the western Tell Atlas, and the Djelfa hunting reserve, located in the Hauts Plateaux (De Smet, 1997; Bounaceur et al., 2016). Overall, despite the species being protected by national law since 1983, the remaining natural populations in northern Algeria are on the verge of extinction (Bounaceur et al., 2016). To the south of the Saharan Atlas, the aoudad occurs in the Provinces of Béchar and Ghardaïa, in the Tademaït Plateau, and in the Provinces of Tamanrasset and Illizi (Kowalski and Rzebik-Kowalska, 1991; De Smet, 1997). Populations in northern Algeria belong to the nominate subspecies *A. l. lervia* (type locality restricted to northwest Algeria by Harper, 1940) (Kowalski and Rzebik-Kowalska, 1991), to which Cassinello et al. (2008) have suggested that the populations in the Provinces of Béchar and Ghardaïa may also belong, whereas *A. l. sahariensis* is the subspecies present in the Tademaït Plateau, close to its type locality (Oued Mya; Rothschild, 1913), and further south in the country (Cassinello et al., 2008) (Fig. 1).

146 The study presented here contributes to our understanding of the geographic
147 genetic structure of the aoudad in Algeria, and the degree of genetic
148 differentiation and the geographic boundaries between the subspecies *A. l. lervia*
149 and *A. l. sahariensis*. We used sequences of the mitochondrial Cytochrome *b* (*Cyt*
150 *b*) gene of aoudad samples collected from the wild in the Algerian Sahara (in
151 both the southeast and west of the country) and from semi-captive and captive
152 populations in the north of Algeria. We also generated and analysed nuclear DNA
153 sequences from four genes (casein kappa, *CSN3*; spectrin beta nonerythrocytic 1,
154 *SPTBN1*; thyroglobulin, *TG*; thyrotropin subunit beta, *TSHB*). These five genes
155 were chosen because they have been used previously in phylogeographic and
156 phylogenetic studies of caprines and other bovids (Matthee and Davis, 2001;
157 Ropiquet and Hassanin, 2006; Hassanin and Ropiquet, 2007; Silva et al., 2017)
158 and because aoudad sequences for these genes are available in public sequence
159 databases. The inclusion of published aoudad sequences allowed us to extend the
160 study to other areas of the species' native range, and to begin investigating its
161 evolutionary history and examining its phylogeography and subspecific
162 taxonomy across its distribution. This knowledge can guide conservation
163 management actions, such as reintroductions, augmentations, and captive
164 breeding.

165

166 **2. Materials and methods**

167 *2.1. Sampling and laboratory procedures*

168 We gathered aoudad samples in Algeria from the wild in the provinces of Béchar
169 in the west and Illizi and Tamanrasset in the southeast, from the semi-captive

populations in the reserves of Djelfa and Moutas and the Cynegetic Centre of Zéralda, and from the Zoological Park of Brabtia d'El Kala (Table 1 and Fig. 1). We are not aware of official information on the origins of the animals in the semi-captive and captive populations; in the literature we only found reference to the origin of the population in the Moutas reserve as being the Algiers Zoo and an enclosure in El Hamma (Bounaceur et al., 2016). In any case, the results of this study are consistent with the hypothesis that aoudads in those semi-captive and captive populations in northern Algeria are derived from individuals caught from wild populations from the same region, which until recently were not as rare as they are today (Kowalski and Rzebik-Kowalska, 1991; Bounaceur et al., 2016). For the semi-captive and captive populations, the samples were muscle tissue from stored specimens, with the exception of the Djelfa Reserve where fresh faecal pellets from each different individual were collected immediately after observation of defecation. Samples from animals in the wild were recently deposited faecal pellet piles (excluding those that appeared to be from more than one individual) collected at sites indicated by local guides and visited and searched immediately after observation with binoculars of aoudads at the sites. Samples were preserved in absolute ethanol and stored at −20 °C. Total genomic DNA was extracted from tissue and faecal samples using the EZNA Tissue DNA kit (Omega Bio-Tek) and the PSP Spin Stool DNA Kit (Stratec), respectively. We amplified a fragment of 775 base pairs (bp) of the *Cyt b* gene with the primers L14724 (5'- TGATATGAAAAACCATCGTTG-3'; Irwin et al., 1991; Rebholz and Harley, 1999) and H15791 (5'- AATGTAGTTGTCTGGGTC-3'; Fernandes et al., 2008). We also amplified fragments of the nuclear genes *CSN3* (736 bp; primers KCAS F2: 5'-GGTTTACATTATGAGCTA-3', and KCAS R: 5'-

195 TTTGATGTCTCCTTAGAG-3'), *SPTBN1* (743 bp; primers SPTBN1 F2: 5'-
196 GTGGAAGACCTGTTACAG-3', and SPTBN1 R: 5'-AAAGCTCTTGGTAACAGA-3'), *TG*
197 (850 bp; primers TG F: 5'-GCCCAAGAAATGTGAGTC-3', and TG R: 5'-
198 AGCACTGTTCTGAGCCTC-3'), and *TSHB* (667 bp; primers TH F: 5'-
199 ATGTGGACAAGCAATGTC-3', and TH R: 5'-CTTGCCACACTTACAGCT-3'). Some of
200 the nuclear primers are from previous studies with slight modifications (KCAS R:
201 Schlieben et al., 1991; SPTBN1 R, TG F and TG R: Ropiquet and Hassanin, 2006),
202 and the remaining ones were newly designed based on alignments of published
203 sequences of Bovidae. Based on data retrieved from the University of California,
204 Santa Cruz (UCSC) Genome Browser (http://genome.ucsc.edu/; Kent et al., 2002;
205 Tyner et al., 2017), the four nuclear genes are located on different chromosomes
206 in cattle (*Bos taurus*) and sheep (*Ovis aries*) (Zimin et al., 2009; Jiang et al., 2014),
207 and thus they may also be unlinked in *A. lervia*. Polymerase chain reactions
208 (PCR) were carried out in volumes of 15 µl with 1x PCR Buffer (Qiagen), 2 mM
209 $MgCl_2$, 0.2 mM of each dNTP (Bioline), 0.5 µM of each primer, 0.6 µg/µl bovine
210 serum albumin (BSA; New England Biolabs), 0.75 U of HotStar Taq DNA
211 Polymerase (Qiagen), and approximately 50 ng of DNA. Thermal cycling
212 conditions consisted of an initial denaturation at 95 °C for 15 min, followed by 45
213 cycles of 30 s at 94 °C, 30 s at 50-55 °C, 1 min at 72°C, and a final extension of 7
214 min at 72°C. The results of the PCR amplifications were visualized on 2% agarose
215 gels to verify PCR quality, and the PCR products were purified with an Exo-SAP
216 protocol (Hanke and Wink, 1994; Werle et al., 1994) and sequenced at Macrogen
217 Inc.
218

219 *2.2. Data analyses*

220 Sequences were edited, assembled and aligned using SEQUENCHER 4.7 (Gene
221 Codes Corporation). We downloaded available aoudad sequences from Genbank
222 and included these in our alignments (Tables 1 and S1). Sequence alignments
223 were analysed with FABOX 1.5 (Villesen, 2007) to identify samples with identical
224 sequences. File format conversions of sequence alignments for use in different
225 computer programs were done using ALTER (Glez-Peña et al., 2010). As shown
226 below in the Results section, variation in the four nuclear genes analysed was
227 extremely low and its distribution across Algeria meant that subsequent
228 analyses of phylogeographic structure would be ineffective; therefore we only
229 performed statistical analyses on the *Cyt b* data.

230 To examine and visualize the genealogical and geographical relationships among
231 the observed mtDNA haplotypes, median-joining networks (Bandelt et al., 1999)
232 were constructed in POPART 1.7 (Leigh and Bryant, 2015). Trimming our *Cyt b*
233 sequences to 627 bp allowed us to include some aoudad *Cyt b* sequences from
234 Genbank, but in order to incorporate additional shorter sequences from diverse
235 geographic origins, we created a smaller alignment of 376 bp (Table 1). The
236 second set of published sequences included 30 samples from Tunisia,
237 corresponding to two haplotypes, and eight samples from Morocco of a single
238 haplotype. We used outgroup rooting (Jansen et al., 2002; Cassens et al., 2003;
239 Dubach et al., 2013) to estimate the ancestral node of the ingroup. We also
240 estimated networks including an ancestral sequence of the aoudad sample
241 studied, as inferred based on a comprehensive phylogenetic dataset of Caprini
242 *Cyt b* sequences (Table S2) and using the marginal reconstruction algorithm of

243 the FASTML web server (http://fastml.tau.ac.il/; Ashkenazy et al., 2012). For
244 comparison, the ancestral sequence was also reconstructed through a Bayesian
245 stochastic character mapping approach implemented in SIMMAP 1.5.2 (Bollback,
246 2006).

247 To assess the presence of mitochondrial clades within *A. lervia* and, if present, to
248 compare their patristic distances to those among other caprine species, we
249 constructed phylogenetic trees based on the above-mentioned Caprini *Cyt b*
250 dataset (Table S2). Prior to tree building, we tested for substitution saturation
251 using the index I_{ss} of Xia et al. (2003) in DAMBE 6.4.40 (Xia, 2017). Substitution
252 saturation was also assessed in DAMBE by plotting the numbers of transitions
253 and transversions against corrected genetic distance for all pairwise sequence
254 comparisons in the dataset, with an asymptotic relationship indicating the
255 presence of saturation. Both the substitution saturation analyses and the tree
256 reconstructions (see below) were conducted considering the *Cyt b* data
257 partitioned by codon position, as this was the best-fit partitioning scheme
258 according to the corrected Akaike information criterion (AICc) (Akaike, 1974;
259 Sugiura, 1978; Hurvich and Tsai, 1989) in PARTITIONFINDER 2.1.1 (Lanfear et al.,
260 2016) using PHYML (Guindon et al., 2010). The corrected genetic distances used
261 in the saturation plots were calculated under the Tamura-Nei model of
262 nucleotide substitution (TN93; Tamura and Nei, 1993), as this was selected by
263 PARTITIONFINDER for each of the codon positions. Phylogenetic analyses were
264 performed using Bayesian inference (BI) and maximum likelihood (ML) as
265 implemented in MRBAYES 3.2.6 (Ronquist et al., 2012) and RAXML 8.2.11
266 (Stamatakis, 2014), respectively. Analyses in MRBAYES were conducted with two
267 parallel runs, each with four Markov chains (one cold and three heated), default

heating parameter (t = 0.1), and 20 million generations. The first five million generations were discarded as burn-in and, thereafter, chains were sampled every 500 generations. The entire general time-reversible (GTR; Lanave et al., 1984) substitution model space was sampled within the analyses (Huelsenbeck et al., 2004). Convergence was indicated by an average standard deviation of split frequencies between parallel runs of less than 0.01. For all model parameters, the effective sample size (ESS) was greater than 900 and the potential scale reduction factor (PSRF) was 1.0. Support for tree nodes was determined according to the values of Bayesian posterior probability (BPP) obtained in a majority-rule consensus tree (Holder et al., 2008; Huggins et al., 2011). In RAxML we used a random starting tree, a GTR + Γ model of sequence evolution for each partition, and support for each node was evaluated by 1000 bootstrap replicates (Felsenstein, 1985). Majority-rule consensus trees (Berry and Gascuel, 1996; Holder et al., 2008) were computed with SumTrees 4.4.0 of the DendroPy library version 4.4.0 (Sukumaran and Holder, 2010) and visualized and edited with FigTree 1.4.4 (available at https://github.com/rambaut/figtree/releases).

Pairwise nucleotide substitution distances between *Cyt b* haplotypes of aoudad and other caprine species were calculated in Mega 10.0.5 (Kumar et al., 2018) under the TN93 model, the one selected from among those available in the software using the Bayesian information criterion (BIC; Schwarz, 1978), and accounting for heterogeneity of substitution pattern among lineages (Tamura and Kumar, 2002). Standard errors (SE) were estimated by bootstrap using 1000 replicates. The TN93 model provides good estimates of genetic distance (d), regardless of nucleotide substitution patterns, when $d < 0.5$ (Tamura and Kumar,

293 2002). Since in studies of mammals, genetic distances for *Cyt b* data are often
294 given as estimated using Kimura's (1980) two-parameter model (K2P) (e.g.
295 Johns and Avise, 1998; Bradley and Baker, 2001), we also calculated K2P
296 distances, again considering uniform substitution rates among sites. For each
297 aoudad mitochondrial clade, we computed the number of segregating sites (S),
298 the number of haplotypes (n_H), haplotype diversity (h), nucleotide diversity (π),
299 Tajima's *D* (Tajima, 1989a) and Fu's F_S (Fu, 1997) in ARLEQUIN 3.5.2.2 (Excoffier
300 and Lischer, 2010). We also calculated in DNASP 5.10.1 (Librado and Rozas,
301 2009) the R_2 statistic (Ramos-Onsins and Rozas, 2002), which may be more
302 powerful than Fu's F_S and Tajima's *D* for detecting demographic growth with
303 small sample sizes (*n*) (Ramos-Onsins and Rozas, 2002; Sano and Tachida, 2005).
304 We did not use tests based on the mismatch distribution (Rogers and
305 Harpending, 1992; Harpending, 1994) because they may have high Type II error
306 rates (Ramos-Onsins and Rozas, 2002).

307 We estimated divergence time between aoudad clades based on net average *Cyt*
308 *b* sequence divergence per site (d_A) (Nei and Li, 1979; Nei, 1987) and using the
309 equation $d_A = 2\mu T$ (Nei, 1987), where μ is the average substitution rate per site
310 and T is the time since divergence. The substitution rate was derived as
311 described in the following. Given our observed *Cyt b* divergence between aoudad
312 and its closest relative, the Arabian tahr, and published estimates of their
313 divergence time (about 5 ± 1 Ma ago) (Ropiquet and Hassanin, 2005a, 2006; Bibi,
314 2013), we obtained a substitution rate using equation $d_{xy} = 2\mu T$, where d_{xy} is the
315 average sequence divergence per site (Nei, 1987). For both intraspecific and
316 interspecific comparisons, sequence divergence calculations were performed in
317 MEGA under the respective best-fit available substitution model selected by BIC.

318 Tajima's test (1993), as implemented in MEGA, was applied to evaluate the
319 assumption of equal rates between aoudad clades, using the Arabian tahr as
320 outgroup, and between aoudad and Arabian tahr, with the Pyrenean chamois
321 *Rupicapra pyrenaica* as outgroup.

322 Divergence time between aoudad *Cyt b* clades was also estimated under two
323 isolation models, one allowing diverging populations to have different initial
324 sizes and varying over time, as implemented in IM (Hey and Nielsen, 2004; Hey,
325 2005), and the other not, conducted in IMa2 (Hey and Nielsen, 2007). Both IM
326 and IMa2 are based on Markov chain Monte Carlo (MCMC) simulations of gene
327 genealogies. In IM we ran 10 Metropolis-coupled chains, with 10 steps between
328 record keeping and 10 genealogy updates per step, for 20 million MCMC steps
329 after a burn-in of one million steps; the scalars for the upper bound on the prior
330 distribution of the θ parameters were 100 and for the upper bound on the prior
331 distribution of the time of population splitting (t) was 60. In IMa2 we also ran 10
332 Metropolis-coupled chains, with 100 steps between genealogy saving, sampling
333 200,000 genealogies after a burn-in of one million steps; the values for the upper
334 bound on the prior distribution of the θ parameters were 500 and for the upper
335 bound on the prior distribution of t was 60. In both IM and IMa2, the upper
336 bounds for the priors of the θ and t parameters were chosen based on
337 preliminary runs with different prior distributions, until they included the tails
338 of the posterior distributions. In the final analyses, we used 45 chain swap
339 attempts per step, a geometric heating scheme, the Hasegawa-Kishino-Yano
340 (HKY) (Hasegawa et al., 1985) nucleotide substitution model, and four
341 independent runs with different starting seeds to verify convergence of
342 parameter estimates. MCMC convergence and mixing of individual runs were

assessed by examination of parameter trend line plots and ESS values. To convert estimates of the time since splitting into years we used the average substitution rate estimate obtained as described above. We also tried to estimate the divergence time between aoudad clades using the coalescent method described by Gaggiotti and Excoffier (2000), as implemented in ARLEQUIN, but the results were not statistically significant. This method aims to remove both the effects of bottlenecks at the time of divergence and unequal genetic drift due to unequal sizes of the descendant populations, as they can lead to overestimation of divergence times from genetic distances, and is robust to population growth after divergence.

We estimated coalescence time of aoudad clades based on Bayesian relaxed phylogenetic analyses of the Caprini *Cyt b* dataset conducted in BEAST 1.8.4 (Drummond et al., 2012). All BEAST input files were created in BEAUti, available in the BEAST package. The alignment was partitioned by codon position, and each partition was analysed using the substitution model selected by JMODELTEST 2.1.10 (Darriba et al., 2012) (according to codon position: TN93 with equal base frequencies + Γ; HKY + I; TN93 + Γ + I). Soft-bound calibration priors were normally distributed with a mean of 10.1 Ma and a standard deviation of 1.5 Ma for the age of the root of the tree, based on published estimates for the age of the clade Caprini + *Pantholops* (Bibi, 2013; see also Ropiquet and Hassanin, 2005a,b and Hassanin et al., 2012), and a mean of 8.9 Ma and a standard deviation of 1.5 Ma for the age of crown Caprini, a calibration point based on the fossil taxon *Aragoral mudejar* (Alcalá and Morales, 1997; Van Dam et al., 2001) and that has been used in previous molecular dating studies of bovids (Pérez et al., 2014; see also Additional File 1 of Bibi, 2013). Note that here we follow Bibi (2013) in

368 excluding *Pantholops* from Caprini as defined by Hassanin and Douzery (1999).
369 Calibrations at deeper nodes generally lead to more accurate and precise rate
370 and date estimates (Duchêne et al., 2014). We also conducted analyses using an
371 additional calibration based on an estimated age of the oldest known *Ovis* fossils
372 at approximately 2.42 Ma (Mead and Taylor, 2005), which again has been used
373 before in divergence time studies of caprines (Ropiquet and Hassanin, 2006;
374 Rezaei et al., 2010). Previous genetic estimates of the time of origin of the genus
375 *Ovis* have ranged between 2.1 and 3.1 Ma (Ropiquet and Hassanin, 2005a;
376 Lalueza-Fox et al., 2005; Bunch et al., 2006; Sanna et al., 2015). The prior on the
377 age of the node was set to a lognormal distribution with a mean of 2.42, log
378 standard deviation of 1.0, and an offset of 1.0. Because the monophyly of Caprini
379 sensu Bibi (2013) is well established (Hassanin et al., 2009; Bibi, 2013), we
380 enforced the monophyly of the group. When calibrated nodes have enforced
381 monophyly, the marginal prior distribution may be a much better match to the
382 calibration density (Heled and Drummond, 2012). Analyses began with a random
383 starting tree, and employed either the Yule process (Yule, 1925; Gernhard, 2008)
384 or the calibrated Yule (Heled and Drummond, 2012) as tree priors; in the latter,
385 the construction of the Yule prior is conditional on calibrated node height. The
386 Yule birth rate prior was set to an exponential distribution with an initial value
387 and mean of 0.3, according to the expected rate for a tree with 39 tips and an
388 assumed height of 10.1 Ma, as calculated using the Python script 'yule.py'
389 (written by Jamie Oaks and available at https://github.com/joaks1/pyule).
390 Substitution rate variation among lineages was modeled with uncorrelated rates
391 drawn from a lognormal distribution (UCLN model, Drummond et al., 2006). The
392 hypothesis of equal evolutionary rate throughout the Caprini *Cyt b* tree was

393 rejected ($P = 1.337 \times 10^{-9}$) by the likelihood ratio test of the molecular clock in
394 MEGA. However, in all the UCLN analyses the estimated coefficient of variation of
395 the branch rates was relatively low (0.112-0.122) and although the 95% highest
396 posterior density (HPD) intervals did not include zero (range: 1.373×10^{-6}-
397 0.299) the frequency histograms were abutting against it, indicating that the data
398 are quite clock-like. In these cases, using a strict molecular clock may increase
399 the precision of divergence date estimates (Ho et al., 2005a; Brown and Yang,
400 2011) and topological inference (Drummond et al., 2006). Therefore, we also
401 performed analyses with a strict clock (SC). Both the priors on the mean branch
402 rate (*ucld.mean*) in the UCLN analyses and on the substitution rate (*clock.rate*) in
403 the SC analyses were set to a broad exponential distribution with an initial value
404 and mean of 0.05. Finally, we set the prior of the relative rates among codon
405 positions to a uniform distribution (0, 1.0E100) with an initial value of 1, the
406 prior on the gamma shape parameter (α) for the third codon position to an
407 exponential distribution with a mean of 10.0 and an initial value of 7.0 (in
408 accordance with the α value estimated by JMODELTEST for third codon positions),
409 and left other priors at default settings. For each combination of calibration
410 points, tree prior and clock model, we ran four independent MCMC analyses,
411 each with 50 million generations and sampled every 5000 generations following
412 a pre-burnin of 10%. We also performed MCMC analyses without sequence data
413 to obtain estimates from the prior distribution and test the influence of priors on
414 posterior distributions (Drummond et al., 2006; Barba-Montoya et al., 2017;
415 Brown and Smith, 2018; Bromham et al., 2018); three independent runs of 50
416 million generations each were carried out under each combination of calibration
417 points, tree prior and clock model. For each analysis, we used TRACER 1.7.1

418 (Rambaut et al., 2018), with a default burn-in of 10% of the chain length, to
419 assess convergence of the chain to the stationary distribution, obtain estimates
420 and ESS of parameters, and plot marginal posterior densities. After verifying
421 convergence, and confirming that posterior distributions of estimates were
422 markedly different from the prior distributions (with the exception of age
423 estimates for the calibration nodes; Brown and Smith, 2018), the tree files from
424 the four runs with data were combined using SUMTREES, with the first 25%
425 (2500) trees from each run discarded as burn-in, into a maximum clade
426 credibility (MCC) tree with median node heights. This method has a good overall
427 performance, in terms of accuracy in estimating ages and model fit, compared to
428 other tree summary approaches (Heled and Bouckaert, 2013; Bromham et al.,
429 2018).

430 Uncorrelated relaxed clock models may underperform in the presence of
431 significant rate autocorrelation among lineages (Lepage et al., 2007; Battistuzzi
432 et al., 2010; Dornburg et al., 2012). We assessed rate autocorrelation in the
433 Caprini *Cyt b* dataset using two methods. First, we examined in TRACER the
434 covariance between parent and child branch rates in the UCLN analyses; if the
435 95% HPD interval for the covariance statistic contains zero, then there is no
436 strong evidence of autocorrelation of rates in the phylogeny (Drummond et al.,
437 2006). However, this method may lack power to detect rate autocorrelation
438 (Battistuzzi et al., 2010; Ho et al., 2015). Hence, we also evaluated rate
439 autocorrelation using a recently developed powerful machine learning method,
440 CorrTest (Tao et al., 2019), available in MEGA.

441 There is now a 'fourth generation' of molecular clock dating approaches (Kumar
442 and Hedges, 2016), which allow rates to vary from branch to branch but do not
443 require prior selection of a statistical model to describe the rate variation or the
444 specification of a branching process model (Kumar and Hedges, 2016). The
445 application of different molecular clock methods allows increasing confidence in
446 the accuracy (i.e. closer to the true divergence time) of congruent results
447 (Battistuzzi et al., 2010; Mello et al., 2017). Thus, times to most recent common
448 ancestor (TMRCA) were also estimated using the RelTime method (Tamura et al.,
449 2012) in MEGA. RelTime is based on a relative rate framework and does not
450 assume either a specific model for lineage rate variation or an underlying
451 diversification process (Battistuzzi et al., 2018; Tamura et al., 2018). It has been
452 benchmarked against Bayesian divergence time analyses, and generally yielded
453 very similar time estimates (Mello et al., 2017). Moreover, it may be particularly
454 useful when the distribution of evolutionary rates differs among clades or when
455 clocks are local (Tamura et al., 2018). The RelTime-ML timetree was computed
456 using a MCC tree with median node heights from the MRBAYES analysis and a
457 TN93 + Γ + I substitution model, the one selected by BIC as the best-fitting
458 among those available in MEGA. The MCC tree had an identical topology to the
459 extended majority-rule consensus tree from the MRBAYES analysis (see below).
460 Analyses were done both using the Caprini MRCA (hard minimum and maximum
461 bounds of 7 and 11 Ma, respectively) as a single calibration constraint or in
462 conjunction with the *Ovis* MRCA (hard minimum and maximum bounds of 1.5
463 and 3.5 Ma, respectively) as an additional calibration. MEGA does not use
464 calibrations located in a clade containing the outgroup(s) because that would

require an assumption of equal rates of evolution between the ingroup and outgroup sequences (Kumar et al., 2016).

3. Results

3.1. Genetic variation, haplotype relationships and phylogenetic analyses

The distinct aoudad DNA sequences generated in this study have been deposited in GenBank under accession numbers MN641980-MN641999 (Tables 1 and S1). From the *Cyt b* sequences, maximizing the number of individuals included as well as sequence length, we obtained an alignment of 702 bp with 39 (5.6%) variable sites, of which 37 (5.3%) were parsimony informative and two (0.3%) were singletons. Several observations indicate that the *Cyt b* sequences produced were mitochondrial and not nuclear-integrated copies of mtDNA (Zhang and Hewitt, 1996; Bensasson et al., 2001). First, the PCR consistently yielded a single product of the expected size. Second, they were unambiguous and highly similar to published homologous sequences of *A. lervia*. Third, they did not contain indels or stop codons. Lastly, they showed a bias against guanine at third codon positions (4% of guanines compared with 24.8 and 14.5% at first and second codon positions, respectively) and against second codon position substitutions (average ML pairwise distance of 0.3% compared with 1% and 9.5% at first and third codon positions, respectively). The four nuclear gene fragments showed low levels of variation. The numbers of polymorphic sites in the samples across Algeria in the analysed fragments of the genes *CSN3*, *SPTBN1*, *TG* and *TSHB* were, respectively, 2, 6, 1 and 2, but in the latter three genes all homozygous individuals at any variable site had the same nucleotide substitution. In fact, for

all nuclear genes there were common haplotypes between northern and southern Algeria (Table S1).

In the median-joining network analysis of *Cyt b* data to investigate phylogeographic patterns in the aoudad, trimming our sequences to 627 bp allowed to include a few sequences from GenBank, but in order to incorporate additional shorter sequences of known geographic origin, a smaller alignment of 376 bp was constructed. The two sets of aoudad sequences contained, respectively, 37 (5.9%) and 24 (6.4%) variable sites, of which 35 (5.6%) and 21 (5.6%) were parsimony informative, and two (0.3%) and three (0.8%) were singletons. The networks revealed two major aoudad phylogroups separated by a large number of mutations (Fig. 2). The minimum number of mutational steps between haplotypes from the two phylogroups in the 627-bp and 376-bp networks was 30 and 16, respectively. The two phylogroups were disconnected in a statistical parsimony analysis (Templeton et al., 1992), even with a relatively liberal connection limit of 0.9 for the probability of parsimony, as implemented in the software TCS (Clement et al., 2000); a result that often indicates the presence of distinct evolutionary lineages in studies using protein-coding mitochondrial genes (Hart and Sunday, 2007). Within Algeria, this main partition can be seen as corresponding to a significant north-south genetic differentiation (Fig. 2a). When the analysis was extended to include published aoudad sequences from other areas in the native range, the general pattern observed appears to actually reflect a Mediterranean-Saharan break (Fig. 2b). One of the two phylogroups was found across the Algerian Sahara (Béchar, Illizi and Tamanrasset provinces), in Niger, and in one specimen in the Mansoura Zoo in Egypt, whereas the other was the only one found in northern Algeria (semi-

514 captive and captive populations), Morocco and Tunisia; the latter phylogroup
515 was also detected in the Béchar Province (Fig. 2b). Given the overall geographic
516 distribution of the two phylogroups, the first is hereafter referred as 'Saharan'
517 and the second as 'Mediterranean'. Based on the 627 bp dataset, the inferred ML
518 ancestral aoudad sequence was more similar to the Saharan phylogroup (Fig. 2a).
519 The ancestral sequence reconstructed using Bayesian character mapping agreed
520 with that estimated by marginal ML reconstruction. Rooting with only the
521 outgroups (Arabian tahr and Pyrenean chamois) also suggest that Saharan
522 phylogroup haplotypes are the most ancestral in the aoudad sample (Fig. S2).

523 To examine for the presence of aoudad clades, we constructed phylogenetic trees
524 based on a comprehensive dataset of Caprini *Cyt b* sequences (Table S2) that
525 were trimmed and added to the aoudad alignment of 702 bp. The resulting
526 alignment had 268 (38.2%) variable sites, of which 209 (29.8%) were parsimony
527 informative and 59 (8.4%) were singletons. Before tree estimation, we tested for
528 substitution saturation. There was no evidence for substantial substitution
529 saturation at any codon position, as the observed I_{ss} was always significantly
530 lower than the critical value (P = 0.00), except for third codon positions when the
531 I_{ss} test was performed assuming an asymmetrical topology ($I_{ss} < I_{ss.cAsym}$, P = 0.18),
532 which clearly does not match the tree we inferred (see below). For each of the
533 three codon positions, the slope and coefficient of determination (r^2) of the
534 linear regression between the numbers of transitions and corrected genetic
535 distance for all pairwise sequence comparisons in the dataset were, respectively:
536 0.86, 0.97; 0.96, 1; 0.18, 0.68. The *Cyt b* BI (Fig. 3) and ML (Fig. S3) consensus
537 trees were very similar. Both topologies recovered the clades *Ammotragus* +
538 *Arabitragus* + *Rupicapra*, *Capra* + *Hemitragus* + *Pseudois* + *Budorcas*, *Nilgiritragus*

539 + *Ovis*, and *Capricornis* + *Naemorhedus* + *Ovibos*, which have been found in
540 previous phylogenetic studies of caprines (Ropiquet and Hassanin, 2005a;
541 Hassanin et al., 2009; Bibi, 2013). In each of the analyses the values of BPP and
542 bootstrap proportions, respectively, strongly supported the two phylogroups
543 inferred from the median-joining network ('Mediterranean' and 'Saharan') as
544 clades. Inspection of the branch lengths in both the BI and ML phylograms
545 indicates that divergence between the two aoudad clades is larger or at least
546 comparable to that among species within *Capra*, *Capricornis*, *Naemorhedus*, *Ovis*,
547 *Pseudois*, or *Rupicapra*. This is confirmed by estimates of genetic distance
548 between sequences under the TN93 (Table S3) and the K2P (Table S4) models.
549 The TN93 pairwise distances, expressed as percent nucleotide substitutions,
550 between the aoudad clades were 4.7-5.4%, while among congeneric species of
551 *Capra* (excluding the problematic *Capra sibirica*, Ropiquet and Hassanin, 2005a,
552 2006), *Capricornis*, *Ovis*, *Pseudois*, and *Rupicapra*, they were, respectively, 2.2-
553 6.0%, 0.6-6.1%, 2.2-6.8%, 1.4%, and 5.3%. The corresponding K2P distances
554 were 4.6-5.4%, 2.2-6.0%, 0.6-6.0%, 2.2-6.7%, 1.4%, and 5.2%, respectively. In
555 terms of amino acid divergence, the numbers of amino acid differences between
556 sequences were 3-5, 2-8, 1-5, 0-3, 2, and 5, respectively (Table S5). Two of the
557 amino acid differences among aoudads were fixed between the Mediterranean
558 and Saharan clades, with phenylalanine versus leucine at residue 121
559 (nucleotide positions 361-363) and alanine versus threonine at residue 122
560 (nucleotide positions 364-366), respectively. At these sites, the amino acid states
561 found in the Saharan clade were identical to those observed in *Arabitragus* and
562 *Rupicapra*.

563 The values of haplotype diversity, nucleotide diversity, Tajima's *D*, Fu's F_S and
564 Ramos-Onsins and Rozas' R_2 for the Mediterranean and Saharan clades were,
565 respectively, as follows: 0.37 ± 0.15, 0.65 ± 0.07; 0.003 ± 0.002, 0.002 ± 0.002; -
566 0.49 (P = 0.35), 0.86 (P = 0.81); 1.48 (P = 0.81), 2.0 (P = 0.86); and 0.13 (P = 0.26),
567 0.20 (P = 0.80) (Table 2). Based on the shorter 376 bp alignment containing
568 more sequences, the values of h, π, Tajima's *D*, Fu's F_S and Ramos-Onsins and
569 Rozas' R_2 for the Mediterranean and Saharan phylogroups were, respectively, as
570 follows: 0.50 ± 0.06, 0.63 ± 0.07; 0.002 ± 0.002, 0.002 ± 0.002; -1.39 (P = 0.07),
571 0.67 (P = 0.79); -2.07 (P = 0.11), 0.45 (P = 0.55); and 0.07 (P = 0.21), 0.19 (P =
572 0.68) (Table 2).

573

574 *3.2. Divergence time estimation*

575 Tajima's test did not reject the hypothesis of equal substitution rates for *Cyt b*
576 among aoudad lineages and Arabian tahr ($P > 0.05$). The estimated *Cyt b* d_{xy}
577 between aoudad and Arabian tahr, using a TN93 + Γ (α = 0.14) substitution
578 model, was 0.171 ± 0.050; approximating the 95% confidence interval (CI) as ± 2
579 SE (e.g. Eizirik et al., 2001; Tchaicka et al., 2007), gives a 95% CI of 0.071-0.271.
580 This *Ammotragus* - *Arabitragus* average divergence, and assuming that they had
581 their MRCA at 5 ± 1 Ma ago, yields a substitution rate of 1.71% per Ma;
582 integrating divergence estimation error and calibration uncertainty results in an
583 overall range for the substitution rate estimate of 0.59-3.39% per Ma. Given the
584 substitution rate of 1.71% per Ma, the estimated d_A between the Mediterranean
585 and Saharan aoudad clades (0.045 ± 0.009; based on the TN93 model; the d_{xy}
586 was 0.050 ± 0.009) corresponds to a divergence time of 1.316 Ma (95% CI:

587 0.789-1.842 Ma). Taking into account the overall uncertainty about the
588 substitution rate (0.59-3.39% per Ma), we obtain the following conservative
589 interval for the divergence time estimate between the two aoudad clades: 0.398-
590 5.339 Ma. Based on the above substitution rate estimate (1.71% per Ma) and
591 using the equation $d_x = 2\mu T$ (Wilson et al., 1985), where d_x is the average
592 pairwise divergence per site within a group of sequences (Nei, 1987), the
593 coalescence times of the clades 'Mediterranean' (d_x = 0.006 ± 0.002) and
594 'Saharan' (d_x = 0.004 ± 0.002) were estimated at 0.175 Ma (95% CI: 0.058-0.292
595 Ma) and 0.117 Ma (95% CI: 0.004-0.234 Ma; lower limit was calculated without
596 rounding the d_x value to three decimal places), respectively. Including the overall
597 uncertainty about the substitution rate (0.59-3.39% per Ma), the respective
598 conservative intervals are 0.029-0.847 Ma and 0.002-0.678 Ma.

599 In the IM and IMa2 analyses, ESS values were > 4150 for each parameter in all
600 individual runs. In the four individual runs in IM, the estimated divergence time
601 between the aoudad clades, taken as the value of the modal smoothed bin in the
602 marginal distribution histogram, ranged from 1.262 to 1.292 Ma (range of 90%
603 HPD intervals: 0.102 - 1,652 Ma). In turn, in the four individual runs in IMa2, the
604 estimated time of divergence between the aoudad clades, also taken as the value
605 of the modal smoothed bin in the marginal distribution histogram, ranged from
606 1.242 to 1.347 Ma (range of the 95% HPD intervals: 0.197 - 1.932 Ma).

607 TMRCAs estimates from the BEAST analyses of *Cyt b* under different
608 combinations of calibrations, tree prior and clock model, are given in Table 3;
609 ESS values were > 3950 for each parameter in all individual runs. All schemes
610 gave similar age estimates and 95% HPD intervals and comparable estimates of

611 mean substitution rate (≈ 1.25-1.37% per Ma) (Table 3). The TMRCA estimates
612 tended to be slightly younger when using three calibration points, i.e. when
613 including the youngest calibration date (2.42 Ma), the one for the origin of the
614 genus *Ovis*; this is in agreement with studies investigating the relationship
615 between estimated mean substitution rate and depth of calibrations (Ho et al.,
616 2005b). We found no evidence of substitution rate autocorrelation among
617 lineages, which if present could make the use of an uncorrelated relaxed clock
618 model less appropriate. In all individual BEAST runs under the UCLN model, the
619 95% HPD interval for the covariance statistic included zero (range of 95% HPD
620 intervals: -0,246 - 0,214). The CorrTest analysis (score of 0.0465) also did not
621 reject the hypothesis of independent evolutionary rates among lineages ($P >$
622 0.05). The fact that the inferred mean substitution rate (≈ 1.25-1.37% per Ma) is
623 consistent with rates estimated for *Cyt b* in previous studies of caprines and
624 other bovids (e.g. Manceau et al., 1999; Lerp et al., 2011) suggests that the
625 calibrations used did not impose an unrealistic evolutionary rate. Moreover, the
626 age estimates for the different nodes in the caprine tree agree well with those in
627 the literature. For example, here is a list of average point estimates that have
628 been obtained (Ropiquet and Hassanin, 2005a; Pérez et al., 2014, 2017) for the
629 TMRCA of some caprine clades: Caprini + *Pantholops*, 9.9-10.7 Ma; Caprini, 8.6-
630 9.7 Ma; *Capricornis* + *Naemorhedus* + *Ovibos*, 5.8 Ma; *Budorcas* + *Pseudois* + *Capra*
631 + *Hemitragus*, 8 Ma; *Capra* + *Hemitragus*, 3.4-4.5 Ma; *Nilgiritragus* + *Ovis*, 3.3-4.5
632 Ma; *Ammotragus* + *Arabitragus* + *Rupicapra*, 6.8-7.9 Ma; *Ammotragus* +
633 *Arabitragus*, 4.6-6 Ma; and *Rupicapra*, 1.5-3.1 Ma. Concerning the genus *Ovis*, its
634 origin has been estimated at 2.1-3.1 Ma (Ropiquet and Hassanin, 2005a; Lalueza-
635 Fox et al., 2005; Bunch et al., 2006; Sanna et al., 2015), the divergence between *O.*

636 *canadensis* and *O. dalli* at 0.9-1.4 Ma (Bunch et al., 2006; Rezaei et al., 2010), the
637 TMRCA of the clade *O. ammon* + *O. a. musimon* + *O. vignei* at 1-1.7 Ma (Bunch et
638 al., 2006; Rezaei et al., 2010; Sanna et al., 2015), and the split between *O. a.*
639 *musimon* + *O. vignei* at 0.9-1.4 Ma (Bunch et al., 2006; Rezaei et al., 2010; Sanna
640 et al., 2015). Finally, the appearance of the ancestor of *Capra* sensu stricto (i.e.
641 excluding *C. sibirica*) and the divergence between *C. ibex* and *C. pyrenaica* have
642 been estimated respectively at 1.5-2 Ma and 0.6-0.7 Ma (Lalueza-Fox et al., 2005;
643 Pérez et al., 2014). The RelTime analyses using either one (Caprini MRCA) or two
644 (Caprini and *Ovis* MRCAs) calibrations produced identical TMRCA point
645 estimates and 95% CIs, except for the latter for nodes directly involving the *Ovis*
646 lineage, which were narrower in the analysis using two calibrations (Table 4).
647 The age estimates from RelTime for nodes across the Caprini phylogeny (Table
648 4) were generally consistent with those from BEAST (Table 3) and those
649 previously published and described above. The confidence intervals from
650 RelTime were broader than those from BEAST, but this could be expected, since
651 the method for estimating confidence intervals in RelTime (Tamura et al., 2012)
652 produces rather wide intervals (Tamura et al., 2018).

653 The BEAST estimates for the TMRCA of the two aoudad clades were 2.6-2.8 Ma
654 (range of 95% HPD intervals: 1.5-4.1 Ma), and for the coalescence of the sampled
655 lineages of each clade were: 'Mediterranean', 0.36-0.39 Ma (range of 95% HPD
656 intervals: 0.14-0.72 Ma); 'Saharan', 0.25-0.27 Ma (range of 95% HPD intervals:
657 0.07-0.56 Ma) (Table 3). In turn, the respective estimates from RelTime were
658 2.34 Ma (95% CI: 1.060-4.055 Ma), 0.098 Ma (95% CI: 0-0.319 Ma), and 0.018
659 Ma (95% CI: 0.006-0.034 Ma) (Table 4).

660

661 **4. Discussion**

662 The aoudad is a threatened species whose native populations are severely
663 fragmented and, in general, show a current declining demographic trend
664 (Cassinello et al., 2008). Moreover, the validity of its subspecies and the true
665 extent of their geographic ranges had not yet been evaluated genetically. The
666 present work focused on the initial investigation of the geographic genetic
667 structure of the aoudad in Algeria, and of the distribution of the subspecies *lervia*
668 and *sahariensis* and their degree of genetic differentiation in that country.
669 However, by including and analysing additional sequences available in public
670 databases of aoudads from other areas of the native distribution in North Africa,
671 our study also has novel potential implications for the subspecific taxonomy of *A.*
672 *lervia*. To our knowledge, this is the first molecular phylogeographic survey of
673 the aoudad and sheds light on the population genetic structure and evolutionary
674 history of the species in its native range. The information provided by this
675 research is also important for aoudad conservation, as it allows for more
676 informed conservation management decisions, in particular regarding
677 reintroductions, reinforcements, translocations, and exchange of individuals
678 among captive stocks (Wyner et al., 1999; Attard et al., 2016).

679 Molecular marker assessments have been invaluable in revealing previously
680 unsuspected deep phylogeographic divergence and major mismatches between
681 inferred genetic units and postulated distribution areas of traditionally
682 recognized subspecies (e.g. Rambau et al., 2003; Mulcahy, 2008). These two
683 phenomena were also observed in the present study. We identified two highly

684 divergent aoudad clades in Algeria (Fig. 2a; mean ML d_A = 4.5%), a partition that
685 the inclusion of published aoudad sequences from other regions in North Africa
686 suggested to be a major phylogeographic split within the native North African
687 range of the species (Fig. 2b; mean ML d_A = 4.7%). In what may be roughly
688 considered a Mediterranean-Saharan break, the 'Mediterranean' clade contained
689 haplotypes found in northern Tunisia, north (in semi-captive and captive
690 populations) and west (in two wild individuals from the Béchar Province)
691 Algeria, and Morocco, and the 'Saharan' clade included haplotypes found in
692 southeast (Illizi and Tamanrasset provinces) and west (in seven wild individuals
693 from the Béchar Province) Algeria, Niger, and Egypt (Mansoura Zoo) (Fig. 2).
694 Notably, the *Cyt b* divergence between the two aoudad clades is greater or at
695 least of the same order of magnitude as those between congeneric species of
696 *Capra*, *Capricornis*, *Naemorhedus*, *Ovis*, *Pseudois*, and *Rupicapra* (Tables S3-S5).
697 Here, however, it should be noted that the alpha taxonomy of *Pseudois* is still
698 under debate, with different authors considering *P. nayaur* and *P. schaeferi* (*Cyt b*
699 sequence divergence of 1.4%) as either distinct species or conspecific (Harris,
700 2014). We also detected two fixed *Cyt b* amino acid differences between the two
701 aoudad clades (Vogler and DeSalle, 1994).

702 *4.1. Phylogeographic history and timing*

703 The age of *A. lervia* was estimated around the Pliocene-Pleistocene boundary
704 (point estimates of 2.6-2.8 Ma from BEAST and ~ 2.3 Ma from RelTime; Tables 3
705 and 4). These estimates roughly agree with the age that has been proposed for
706 what are, to our knowledge, the oldest *Ammotragus* fossils in Africa

(Villafranchian of Mechta-el-Arbi, Algeria) (Romer, 1928; Hopwood and Hollyfield, 1954).

Point estimates for the divergence time between the two aoudad clades from either d_A, IM or IMa2, were consistently close to 1.3 Ma. This is encouraging (Fu and Li, 1999) because the three methods are very different in terms of the underlying demographic models, assumptions, and algorithms used. For instance, the distance d_A assumes that the sizes of the derived populations are equal and constant over time, that is, they experience the same genetic drift. Similarly, IMa2 assumes that descendant populations are of constant size, but in IM we used a model in which descendant populations may have different initial sizes and subsequent independent demographic histories in which population growth or shrinkage is allowed. Using models that consider the possibility of different sizes of the daughter populations can significantly reduce bias in divergence time estimates (Gaggiotti and Excoffier, 2000). It is also known that demographic bottlenecks can increase genetic distances between populations (Wilson et al., 1985; Gaggiotti and Excoffier, 2000), but this bottleneck effect may be less when population divergence is large and within-population genetic diversity is limited (Takezaki and Nei, 1996; Hedrick, 1999; Gaggiotti and Excoffier, 2000), especially if, as we did, one uses models explicitly accounting for unequal-sized daughter populations (Gaggiotti and Excoffier, 2000). The estimated divergence time between the two aoudad clades of about 1.3 Ma corresponds approximately to the beginning of a long period (~ 100 ka) without 'green Sahara' episodes (Larrasoaña et al., 2013; Rohling et al., 2015), during which there must have been fragmentation of the aoudad's geographic distribution. This vicariance may

731 have led to allopatric divergence between aoudad populations in distant regions
732 separated by barriers and beyond their dispersal capacities (Gray and Simpson,
733 1980), and this could explain the two highly distinct major clades observed
734 (Avise et al., 1987). Despite the inferred ancient ancestry for both clades, the low
735 levels of genetic variation and the genealogical and geographic patterns within
736 each of the two clades (Fig. 2) suggest a relatively recent coalescence of their
737 extant diversity, which we interpret as the result of strong historical population
738 bottlenecks (Maruyama and Fuerst, 1985; Wilson et al., 1985; Avise et al., 1988;
739 Grant and Bowen, 1998). These were apparently followed by regional range
740 expansions over long distances of the two lineages (Neigel and Avise, 1993),
741 which would explain the presence of the 'Mediterranean' clade in Morocco,
742 northern Algeria, and Tunisia, and the 'Saharan' clade in Egypt, Niger, and
743 southeastern Algeria. Indeed, a haplotype found in northern Algeria is also
744 present in Tunisia and the haplotype detected in Morocco differs from that one
745 by a single nucleotide substitution, and a haplotype found in southeastern
746 Algeria was also recovered in Niger and Egypt (Fig. 2b). Concordantly, based on
747 the 702 bp alignment, the estimated average nucleotide and haplotype diversity
748 were low and moderate, respectively, in both clades ('Mediterranean': n = 15, π =
749 0.3%, h = 0.37; 'Saharan': n = 15, π = 0.2%, h = 0.65) (Table 2), which are
750 patterns that can be considered consistent in both cases with a history of
751 population bottleneck followed by population growth and expansion (Grant and
752 Bowen, 1998). This conclusion holds when considering the shorter 376 bp
753 alignment including GenBank sequences, in particular of aoudads from Morocco,
754 Tunisia and Niger ('Mediterranean': n = 67, π = 0.2%, h = 0.50; 'Saharan': n = 17,
755 π = 0.2%, h = 0.63) (Table 2). The fact that the Tajima's D, Fu's F_S and Ramos-

Onsins and Rozas' R_2 tests did not indicate demographic growth may be due to a lack of power because of the small numbers of segregating sites (Ramos-Onsins and Rozas, 2002), or because the expansion of the clades was relatively recent, since it has been shown that under realistic population growth models these tests may have more power to detect older expansions (Fu, 1997; Ramos-Onsins and Rozas, 2002). Alternatively, given the negative and closer to statistically significant values of D and F_S for the 'Mediterranean' clade in the 376 bp alignment (Table 2), one might think that larger sample sizes could detect expansion signatures; however, the power of the F_S and R_2 tests can reach 0.7-0.8 for n = 15 (Ramos-Onsins and Rozas, 2002). Overall, the reason why the three mutation-drift equilibrium tests used did not identify expansion signals may have been a combination of few segregating sites and moderate sample sizes (Ramos-Onsins and Rozas, 2002). The high nucleotide diversity and high positive values of Tajima's D and Fu's F_S for the overall sets of aoudad *Cyt b* sequences (Table 2), especially for the longer 702 bp alignment, are interpreted as due to the deep phylogeographic break in the species (Simonsen et al., 1995; Grant and Bowen, 1998).

Geographic expansion of formerly allopatric and isolated populations may lead to their secondary contact (Avise et al., 1987); if since then gene flow has been sufficiently restricted, the lineages from the different former isolates may still have limited overlap in their distribution (Templeton et al., 1995). This is what we detected, with the presence of the two clades in the Béchar Province (Fig. 2). This region is adjacent to southeastern Morocco and the western end of the Saharan Atlas, but is connected by the Saoura Valley and rocky plateaus to the

780 Tademaït in central Algeria and through it to the Illizi and Tamanrasset
781 provinces in southeastern Algeria. Additional sampling, in particular from
782 regions not yet sampled such as Mauritania, Mali and Libya, is needed to better
783 define geographic boundaries of clades and to verify the existence or otherwise
784 of other areas of apparent sympatry or parapatry.

785 Assuming that the *Cyt b* substitution rate calibrated with the *Ammotragus-*
786 *Arabitragus* divergence may be more appropriate than the average substitution
787 rates estimated in the BEAST analyses to date coalescence events within the
788 aoudad (Thorne et al., 1998), the mean coalescence times estimated in the
789 BEAST analyses for extant genetic diversity in the 'Mediterranean' and 'Saharan'
790 clades can be tentatively converted to approximately 287 ka and 199 ka,
791 respectively. This, together with the respective mean estimates from d_x (175 ka
792 and 117 ka), suggests coalescences around the Middle-Late Pleistocene. On the
793 other hand, considering that short-term mutation rates may be measurably
794 higher than phylogenetic estimates of substitution rates (Ho et al., 2005b, 2007,
795 2011), this raises the possibility that coalescences date to the Last Glacial Period
796 (~ 115-12 ka), as hinted at by the estimates from RelTime. In addition to
797 uncertainty about the short-term substitution rate, age estimates of the extant
798 genetic diversity of clades may be particularly sensitive and dependent on
799 sample size, and therefore these results should be confirmed with additional
800 sampling as this may reveal more haplotypes. However, the single sample from
801 Egypt showed the same haplotype as the single sample from Niger, and this
802 haplotype was also the most common in samples from southeastern Algeria.
803 Moreover, almost all samples from Tunisia and northern Algeria shared the same

haplotype, and all eight samples from Morocco exhibited the same haplotype (Fig. 2). Thus, there may not be much more mitochondrial diversity to be found in each clade because when bottlenecks are strong and relatively recent, and given the relatively modest substitution rate of *Cyt b*, mitochondrial variation (particularly nucleotide diversity) may still be very low (Maruyama and Fuerst, 1984, 1985; Wilson et al., 1985; Tajima, 1989b; Björklund, 2003) so that it is essentially captured even with only moderate sample sizes.

4.2. Taxonomic and conservation considerations

This study revealed the presence of two highly differentiated mitochondrial lineages in the aoudad, with a level of *Cyt b* divergence greater than or comparable to those observed between several pairs of congeneric species of different Caprini genera. The two lineages were mostly allopatric, with one being present in Morocco, northern Algeria and Tunisia, and the other in southeastern Algeria, Niger and Egypt, with the exception of one apparent contact zone in western Algeria (Béchar). These genetic and geographic patterns, accompanied by the fact that the division seemingly corresponds to a history of ecological separation between temperate Mediterranean and arid Saharan regions, suggest the presence of two subspecies in the data analysed (O'Brien and Mayr, 1991). This hypothesis should be evaluated with analyses using detailed sampling covering the Saharan distribution of the aoudad, and also based on other evidence not yet available, such as informative markers from the nuclear genome (Avise and Ball, 1990; Zhang and Hewitt, 2003), molecular cytogenetic comparisons (Rambau et al., 2003; Adega et al., 2018), and geometric morphometric data (Evin et al., 2008). Interestingly, the phylogeographic

828 subdivision we detected in Algeria roughly agrees with the distribution
829 discussed by Cassinello et al. (2008) for the subspecies *lervia* and *sahariensis* in
830 that country, with uncertainty as to the subspecies present in Béchar. On the
831 other hand, our results do not appear to be consistent with the distinction
832 between the subspecies *sahariensis*, *angusi* and *ornata*, as samples from
833 respectively southeastern Algeria, Niger and Egypt shared the same haplotype
834 (Fig. 2).

835 Irrespective of issues of subspecies taxonomy and distinction between *lervia* and
836 *sahariensis*, the Mediterranean and Saharan aoudad populations appear to be
837 two distinct evolutionary units (Ryder, 1986; Zink, 2004) with a long history of
838 geographic isolation (Moritz, 2002) and likely adaptive divergence in response
839 to contrasting ecological conditions (Lynch et al., 1999; Merilä and Crnokrak,
840 2001). Therefore, the conservation of both units is essential, and their
841 management should be independent to maintain evolutionary potential across
842 heterogenous environments (O'Brien and Mayr, 1991; Moritz, 1994, 2002;
843 Fraser and Bernatchez, 2001). In this latter context, it is worth noting that the
844 commonly held view that the captive population at the Experimental Station of
845 Arid Zones (EEZA; Almería, Spain) belongs to the subspecies *sahariensis*
846 (Cassinello, 1998) is not supported by our study.

847

848 **5. Conclusions**

849 Mitochondrial genes, due to their typically higher variability and rate of genetic
850 drift (Brown et al., 1979; Moritz et al., 1987; Pesole et al., 1999), can be more
851 powerful and informative than nuclear genes for inferring population

852 genealogical patterns and demographic history within animal species (Wilson et
853 al 1985; Moore, 1995; Zink and Barrowclough, 2008; Barrowclough and Zink,
854 2009). This study highlights the value of mtDNA, probably unrivalled by any
855 other single-locus marker, as an exploratory tool to investigate and uncover
856 historical genetic structure, assess subspecific taxonomy, and identify potential
857 evolutionarily significant units for conservation (Avise, 1989, 1995; Harrison,
858 1989; Lerp et al., 2011; Andersen and Light, 2012; Derouiche et al., 2017; Prieto-
859 Torres et al., 2018). In agreement, none of the four nuclear genes that we also
860 surveyed, chosen because they have already been used in phylogeographic and
861 species-level phylogenetic studies of bovids, allowed us to detect any
862 unambiguous sign of the substantial and geographically coherent intraspecific
863 subdivision exposed by mtDNA. This is likely due to their slow evolutionary rate
864 (Matthee and Davis, 2001).

865 This first phylogeographic survey of the aoudad indicated a deep Mediterranean-
866 Saharan genetic break in the species, suggesting the presence of two highly
867 distinct evolutionary lineages. It therefore highlights and raises the profile of this
868 threatened and poorly studied ungulate emblematic of the North African
869 landscape for further phylogeographic and taxonomic research with improved
870 geographic sampling across the species' range, and using other types of nuclear
871 markers such as fast-mutating microsatellites (Charruau et al., 2011; Buchalski
872 et al., 2016) or genome-wide panels of single nucleotide polymorphisms (SNPs)
873 (Sim et al., 2016; Dotsev et al., 2018).

874

875

Figures and Tables

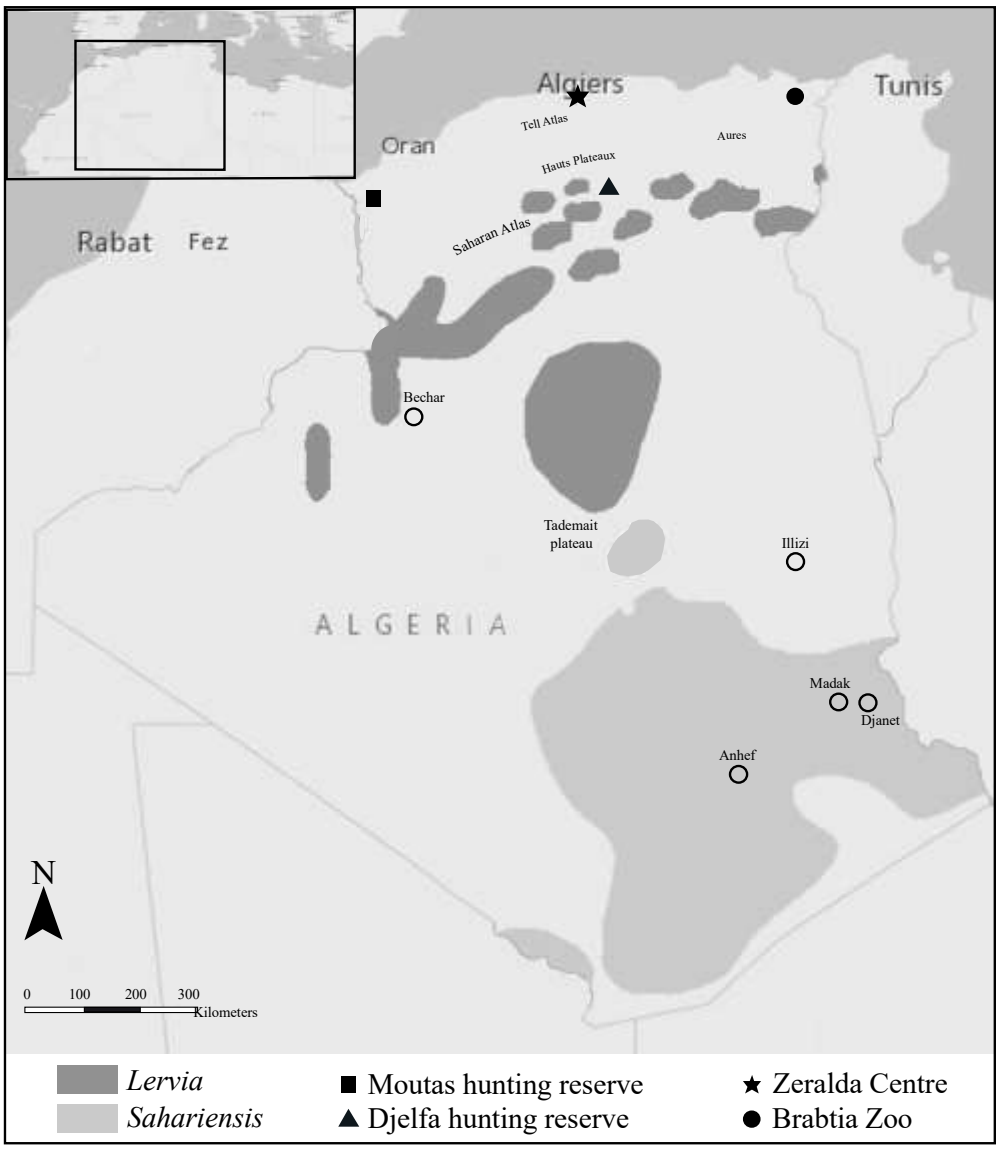

Fig. 1. Map showing the locations in Algeria where aoudad samples were collected for this study (see Table 1 for details). The black symbols indicate the semi-captive and captive populations in northern Algeria and the black open circles represent locations of samples from wild populations. Also shown are the possible distribution areas described in Cassinello et al. (2008) for the two aoudad subspecies recognized in Algeria. Major toponyms are also indicated. The inset shows Algeria's position in northwest Africa and in the Mediterranean region.

Table 1. Information on the aoudad samples and *Cyt b* sequences used in this study. An asterisk (*) indicates countries where the species is non-native.

Sample code	Country	Sampling location	Haplotype (702 bp alignment)	Haplotype (627 bp alignment)	Haplotype (376 bp alignment)	GenBank accession number	Reference
M2	Algeria	Moutas Reserve	H1	H1	H1	MN641980	This study
M3	Algeria	Moutas Reserve	H1	H1	H1	MN641980	This study
M7	Algeria	Moutas Reserve	H1	H1	H1	MN641980	This study
M8	Algeria	Moutas Reserve	H1	H1	H1	MN641980	This study
M9	Algeria	Moutas Reserve	H1	H1	H1	MN641980	This study
M10	Algeria	Brabtia Zoo	H1	H1	H1	MN641980	This study
M11	Algeria	Béchar Province	H2	H2	H5	MN641981	This study
M14	Algeria	Illizi District	H3	H3	H6	MN641982	This study
M15	Algeria	Béchar Province	H2	H2	H5	MN641981	This study
M16	Algeria	Béchar Province	H2	H2	H5	MN641981	This study
M17	Algeria	Béchar Province	H2	H2	H5	MN641981	This study
M18	Algeria	Béchar Province	H2	H2	H5	MN641981	This study
M19	Algeria	Béchar Province	H4	H4	H7	MN641983	This study
M20	Algeria	Béchar Province	H2	H2	H5	MN641981	This study
M21	Algeria	Béchar Province	H2	H2	H5	MN641981	This study
M22	Algeria	Zéralda Centre		H1	H1		This study
M23	Algeria	Béchar Province	H5	H5	H7	MN641984	This study
M25	Algeria	Djanet District	H3	H3	H6	MN641982	This study
M26	Algeria	Madak, Djanet District	H3	H3	H6	MN641982	This study
M27	Algeria	Madak, Djanet District	H6	H6	H8	MN641985	This study

Sample code	Country	Sampling location	Haplotype (702 bp alignment)	Haplotype (627 bp alignment)	Haplotype (376 bp alignment)	GenBank accession number	Reference
M28	Algeria	Madak, Djanet District	H3	H3	H6	MN641982	This study
M29	Algeria	Madak, Djanet District	H6	H6	H8	MN641985	This study
M31	Algeria	Anhef, Tamanrasset Province	H3	H3	H6	MN641982	This study
1_Djelfa	Algeria	Djelfa Reserve	H1	H1	H1	MN641980	This study
2_Djelfa	Algeria	Djelfa Reserve		H1	H1		This study
3_Djelfa	Algeria	Djelfa Reserve	H1	H1	H1	MN641980	This study
4_Djelfa	Algeria	Djelfa Reserve	H1	H1	H1	MN641980	This study
5_Djelfa	Algeria	Djelfa Reserve	H1	H1	H1	MN641980	This study
6_Djelfa	Algeria	Djelfa Reserve	H1	H1	H1	MN641980	This study
7_Djelfa	Algeria	Djelfa Reserve	H1	H1	H1	MN641980	This study
	Egypt	Mansoura Zoo	H3	H3	H6	EF466060	Mereu et al. 2008
	Niger				H6	= EF466060	Silva et al. 2015
	Algeria	Semi-captive in northern Algeria			H1	KM582123	Silva et al. 2015
	Algeria	Semi-captive in northern Algeria			H2	KM582126	Silva et al. 2015
	Algeria	Semi-captive in northern Algeria			H3	KM582125	Silva et al. 2015
	Tunisia				H4	KM582124	Silva et al. 2015
	Tunisia				H1	KM582123	Silva et al. 2015
	Morocco				H9	= FJ207522	Silva et al. 2015
	Spain*	"La Hoya" Field Station, Almería			H9	= FJ207522	Silva et al. 2015
	Spain*	"La Hoya" Field Station, Almería			H1	KM582123	Silva et al. 2015

Sample code	Country	Sampling location	Haplotype (702 bp alignment)	Haplotype (627 bp alignment)	Haplotype (376 bp alignment)	GenBank accession number	Reference
		Vincennes Zoo, Paris	H7	H8	H9	FJ207522	Hassanin et al. 2009
		MNHN, Paris		H8	H9	AF034731	Hassanin et al. 1998
				H1	H1	FJ556568	Unpublished
				H7	H5	KU165683	Unpublished

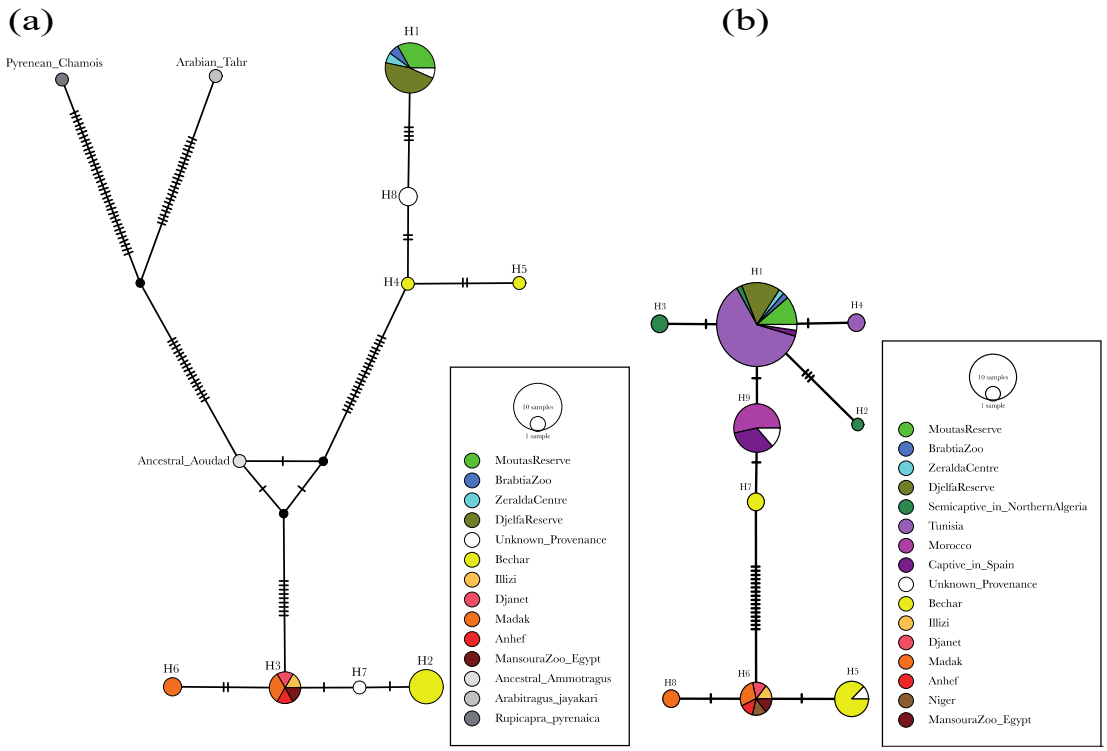

Fig. 2. Median-joining networks of (a) 627-bp and (b) 376-bp aoudad *Cyt b* haplotypes. The first contains 35 aoudad sequences and is rooted with two outgroups, Arabian tahr and Pyrenean chamois, and an inferred ancestral aoudad sequence; the second contains 84 aoudad sequences. Circles represent haplotypes and their size is proportional to frequency. Circles are coloured according to where haplotypes were found and to their relative frequency. Small black circles represent hypothetical haplotypes. Dashes on lines connecting haplotypes represent the number of nucleotide substitutions separating them. Haplotype designations and further information are given in Table 1.

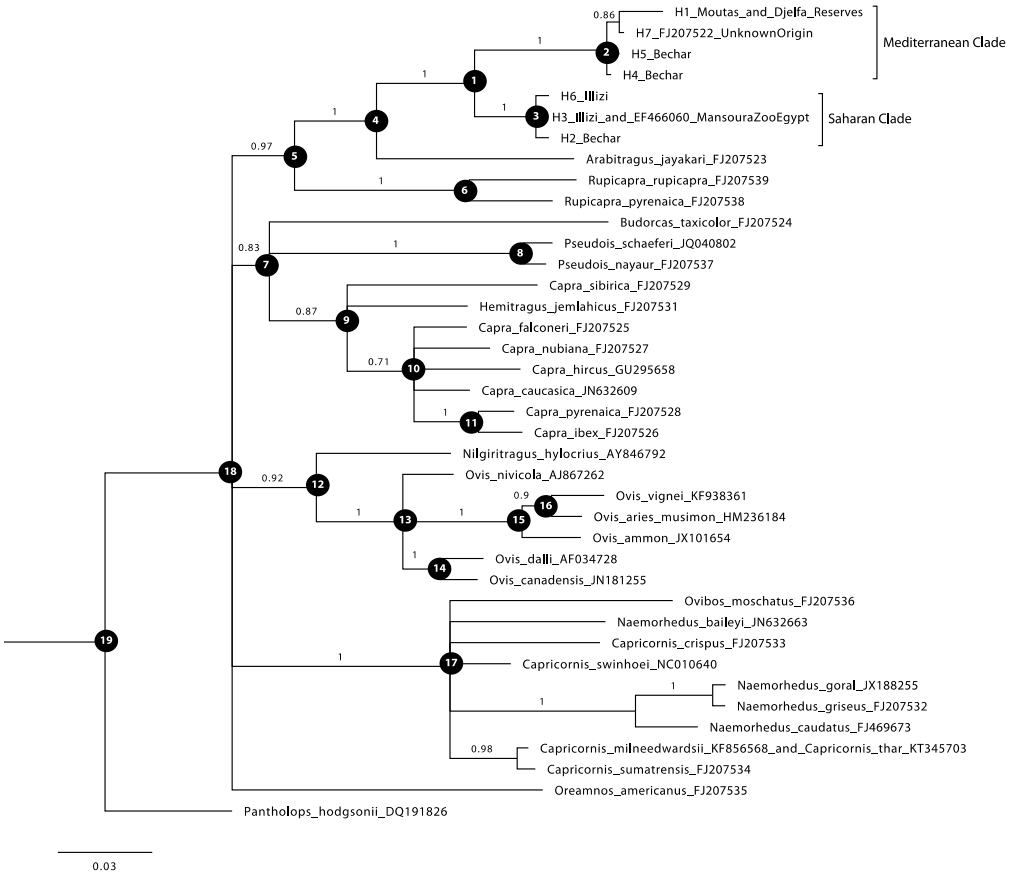

Fig. 3. Majority-rule consensus phylogram (cut-off 0.7) from the Bayesian inference analysis of the 702-bp caprine *Cyt b* haplotypes. See Tables 1 and S2 for haplotype information. Numbers above branches are Bayesian posterior probabilities. Numbers within black circles at nodes are keyed to the numbers in the first column of Tables 3 and 4. The identified 'Mediterranean' and 'Saharan' aoudad clades are also indicated.

Table 2. Estimates of genetic diversity and mutation-drift equilibrium tests for the overall sets of aoudad *Cyt b* sequences analysed and for each of the two clades identified in this study, based on two alignments with different sequences and lengths.

	S	**n_H**	**h**	**π**	***D***	***F_s***	***R_2***
Overall							
702 bp dataset (n = 30)	39	7	0.763 ± 0.051	0.025 ± 0.013	2.904 (P = 1.000)	13.227 (P = 1.000)	0.224 (P = 1.000)
376 bp dataset (n = 84)	24	9	0.671 ± 0.048	0.017 ± 0.009	1.035 (P = 0.883)	6.400 (P = 0.954)	0.133 (P = 0.899)
Mediterranean Clade							
702 bp dataset (n = 15)	8	4	0.371 ± 0.153	0.003 ± 0.002	-0.489 (P = 0.348)	1.484 (P = 0.807)	0.132 (P = 0.264)
376 bp dataset (n = 67)	7	6	0.503 ± 0.060	0.002 ± 0.002	-1.394 (P = 0.066)	-2.074 (P = 0.106)	0.066 (P = 0.205)
Saharan Clade							
702 bp dataset (n = 15)	4	3	0.648 ± 0.072	0.002 ± 0.002	0.864 (P = 0.809)	1.997 (P = 0.864)	0.195 (P = 0.800)
376 bp dataset (n = 17)	2	3	0.632 ± 0.066	0.002 ± 0.002	0.669 (P = 0.785)	0.446 (P = 0.552)	0.188 (P = 0.682)

n, number of samples; S, number of segregating sites; n_H, number of haplotypes; h, haplotype diversity; π, nucleotide diversity; *D*, Tajima's *D* statistic (Tajima, 1989a); F_S, Fu's F_S statistic (Fu, 1997); R_2, Ramos-Onsins and Rozas' R_2 statistic (Ramos-Onsins and Rozas, 2002); P, *p*-value of the test.

Table 3. TMRCA point estimates (medians of the posterior distributions) and 95% highest posterior density (HPD) intervals, in millions of years ago (Ma), from the BEAST analyses of *Cyt b* using different tree priors (Yule or calibrated Yule) and clock models (UCLN or strict) and two or three calibration points. The numbers in the first column correspond to the node numbers in Figure 3.

Node in Fig. 3	Clade/Split	Point estimates; 95% HPD intervals			
		Yule; UCLN 2 calibration points	**Yule; strict clock 2 calibration points**	**Calibrated Yule; UCLN 2 calibration points**	**Calibrated Yule; strict clock 2 calibration points**
1	*A. lervia*	2.620; 1.598 - 3.827	2.664; 1.699 - 3.800	2.804; 1.634 - 4.120	2.837; 1.749 - 4.078
2	'Mediterranean' aoudad	0.372; 0.149 - 0.666	0.369; 0.158 - 0.651	0.394; 0.165 - 0.720	0.392; 0.169 - 0.712
3	'Saharan' aoudad	0.255; 0.067 - 0.528	0.256; 0.074 - 0.527	0.272; 0.068 - 0.560	0.272; 0.072 - 0.555
4	*Ammotragus* + *Arabitragus*	4.859; 3.262 - 6.665	4.950; 3.394 - 6.636	5.193; 3.432 - 7.229	5.245; 3.542 - 7.179
5	*Ammotragus* + *Arabitragus* + *Rupicapra*	6.822; 4.868 - 8.861	6.903; 5.019- 8.871	7.240; 5.058- 9.552	7.298; 5.193- 9.575
6	*Rupicapra*	2.311; 1.285 - 3.489	2.329; 1.456 - 3.447	2.456; 1.382 - 3.782	2.475; 1.461 - 3.666
7	*Budorcas* + *Pseudois* + *Capra* + *Hemitragus*	7.105; 5.205 - 8.975	*	7.527; 5.390 - 9.727	*
8	*Pseudois*	0.557; 0.222 - 0.992	0.557; 0.249 - 0.969	0.593; 0.233 - 1.057	0.591; 0.244 - 1.025
9	*Capra* + *Hemitragus*	4.783; 3.235 - 6.537	4.839; 3.398 - 6.533	5.104; 3.368 - 7.114	5.148; 3.503 - 7.064
10	*Capra* sensu stricto	2.382; 1.600 - 3.315	2.377; 1.625 - 3.230	2.539; 1.649 - 3.597	2.537; 1.714 - 3.517
11	*C. ibex* + *C. pyrenaica*	0.818; 0.401 - 1.325	0.829; 0.432 - 1.311	0.872; 0.428 - 1.436	0.881; 0.450 - 1.412
12	*Nilgiritragus* + *Ovis*	4.539; 3.038 - 6.215	4.487; 3.054 - 6.035	4.821; 3.085 - 6.657	4.763; 3.219 - 6.539
13	*Ovis*	3.066; 2.088 - 4.279	3.077; 2.153 - 4.195	3.265; 2.090 - 4.551	3.269; 2.175 - 4.468
14	*O. canadensis* + *O. dalli*	0.889; 0.440 - 1.461	0.895; 0.461 - 1.434	0.950; 0.445 - 1.576	0.953; 0.475 - 1.538
15	*O. ammon* + *O. a. musimon* + *O. vignei*	1.331; 0.798 - 1.991	1.342; 0.806 - 1.945	1.414; 0.821 - 2.154	1.427; 0.861 - 2.108
16	*O. a. musimon* + *O. vignei*	0.874; 0.436 - 1.404	0.885; 0.486 - 1.409	0.929; 0.446 - 1.490	0.939; 0.498 - 1.500
17	*Capricornis* + *Naemorhedus* + *Ovibos*	5.246; 3.816 - 6.777	5.369; 4.005 - 6.860	5.553; 3.972 - 7.358	5.661; 4.100 - 7.371
18	Caprini	9.211; 7.424 - 10.875	9.270; 7.506 - 10.967	9.575; 7.421 - 11.685	9.641; 7.540 - 11.758
19	Caprini + *Pantholops*	9.760; 8.077 - 11.572	9.732; 8.003 - 11.472	10.006; 7.942 - 12.095	10.009; 7.905 - 12.038
	Estimated mean substitution rate	1.33%	1.32%	1.26%	1.25%

* Asterisks indicate nodes not recovered with BPP ≥ 0.8 in the respective MCC tree.

(*Cont.*)

Table 3. (*Cont.*)

Node in Fig. 3	Clade/Split	Point estimates; 95% HPD intervals			
		Yule; UCLN 3 calibration points	**Yule; strict clock 3 calibration points**	**Calibrated Yule; UCLN 3 calibration points**	**Calibrated Yule; strict clock 3 calibration points**
1	*A. lervia*	2.557; 1.529 - 3.730	2.601; 1.654 - 3.688	2.701; 1.610 - 4.010	2.736; 1.687 - 3.950
2	'Mediterranean' aoudad	0.360; 0.138 - 0.639	0.360; 0.151 - 0.637	0.378; 0.152 - 0.690	0.377; 0.151 - 0.669
3	'Saharan' aoudad	0.248; 0.066 - 0.508	0.249; 0.069 - 0.502	0.262; 0.075 - 0.547	0.262; 0.071 - 0.535
4	*Ammotragus* + *Arabitragus*	4.762; 3.201 - 6.613	4.829; 3.367 - 6.569	5.018; 3.268 - 6.989	5.076; 3.386 - 6.964
5	*Ammotragus* + *Arabitragus* + *Rupicapra*	6.698; 4.796 - 8.772	6.735; 4.920 - 8.747	7.019; 4.895 - 9.285	7.056; 4.981 - 9.266
6	*Rupicapra*	2.256; 1.293 - 3.434	2.267; 1.382 - 3.339	2.370; 1.337 - 3.660	2.383; 1.411 - 3.528
7	*Budorcas* + *Pseudois* + *Capra* + *Hemitragus*	6.912; 5.181 - 8.950	*	*	*
8	*Pseudois*	0.542; 0.223 - 0.975	0.542; 0.241 - 0.942	0.571; 0.234 - 1.033	0.569; 0.248 - 0.998
9	*Capra* + *Hemitragus*	4.663; 3.105 - 6.366	4.712; 3.298 - 6.388	4.930; 3.238 - 6.855	4.960; 3.370 - 6.826
10	*Capra* sensu stricto	2.314; 1.564 - 3.228	2.310; 1.590 - 3.158	2.447; 1.588 - 3.484	2.440; 1.634 - 3.383
11	*C. ibex* + *C. pyrenaica*	0.797; 0.393 - 1.299	0.803; 0.405 - 1.259	0.838; 0.394 - 1.377	0.848; 0.443 - 1.380
12	*Nilgiritragus* + *Ovis*	4.356; 2.934 - 6.011	4.316; 2.981 - 5.842	4.579; 3.051 - 6.487	4.541; 3.029 - 6.235
13	*Ovis*	2.833; 1.961 - 3.973	2.900; 2.027 - 3.939	3.037; 1.958 - 4.219	3.049; 2.047 - 4.178
14	*O. canadensis* + *O. dalli*	0.858; 0.412 - 1.406	0.860; 0.443 - 1.375	0.908; 0.441 - 1.515	0.907; 0.459 - 1.464
15	*O. ammon* + *O. a. musimon* + *O. vignei*	1.274; 0.755 - 1.898	1.288; 0.790 - 1.875	1.342; 0.776 - 2.033	1.353; 0.825 - 2.014
16	*O. a. musimon* + *O. vignei*	0.836; 0.423 - 1.349	0.850; 0.462 - 1.352	0.883; 0.428 - 1.427	0.894; 0.463 - 1.412
17	*Capricornis* + *Naemorhedus* + *Ovibos*	5.141; 3.768 - 6.694	5.252; 3.963 - 6.755	5.384; 3.801 - 7.120	5.475; 3.948 - 7.150
18	Caprini	9.049; 7.280 - 10.789	9.096; 7.379 - 10.817	9.322; 7.120 - 11.399	9.361; 7.281 - 11.470
19	Caprini + *Pantholops*	9.616; 7.850 - 11.392	9.558; 7.850 - 11.343	9.770; 7.630 - 11.785	9.742; 7.694 - 11.842
	Estimated mean substitution rate	1.37%	1.36%	1.31%	1.30%

* Asterisks indicate nodes not recovered with BPP ≥ 0.8 in the respective MCC tree.

Table 4. TMRCA point estimates and 95% confidence intervals (CI), in millions of years ago (Ma), from the RelTime analyses of *Cyt b* using one or two calibration points. The numbers in the first column correspond to the node numbers in Figure 3.

Node in Fig. 3	Clade/Split	Point estimates; 95% CI	
		One calibration point: Caprini	**Two calibration points: Caprini; *Ovis***
1	*A. lervia*	2.340; 1.060 - 4.055	2.340; 1.060 - 4.055
2	'Mediterranean' aoudad	0.098; 0 - 0.319	0.098; 0 - 0.319
3	'Saharan' aoudad	0.018; 0.006 - 0.034	0.018; 0.006 - 0.034
4	*Ammotragus* + *Arabitragus*	4.735; 2.734 - 7.278	4.735; 2.734 - 7.278
5	*Ammotragus* + *Arabitragus* + *Rupicapra*	6.498; 3.979 - 9.633	6.498; 3.979 - 9.633
6	*Rupicapra*	2.488; 1.215 - 4.173	2.488; 1.215 - 4.173
7	*Budorcas* + *Pseudois* + *Capra* + *Hemitragus*	7.225; 4.463 - 10.649	7.225; 4.463 - 10.649
8	*Pseudois*	0.581; 0.088 - 1.283	0.581; 0.088 - 1.283
9	*Capra* + *Hemitragus*	4.686; 2.757 - 7.122	4.686; 2.757 - 7.122
10	*Capra* sensu stricto	2.134; 1.071 - 3.533	2.134; 1.071 - 3.533
11	*C. ibex* + *C. pyrenaica*	0.728; 0.182 - 1.493	0.728; 0.182 - 1.493
12	*Nilgiritragus* + *Ovis*	5.380; 3.193 - 8.134	5.380; 3.198 - 8.127
13	*Ovis*	2.736; 1.439 - 4.427	2.736; *1.5 - 3.5*
14	*O. canadensis* + *O. dalli*	1.380; 0.471 - 2.631	1.380; 0.620 - 2.398
15	*O. ammon* + *O. a. musimon* + *O. vignei*	0.904; 0.306 - 1.729	0.904; 0.386 - 1.604
16	*O. a. musimon* + *O. vignei*	0.532; 0.116 - 1.118	0.532; 0.165 - 1.041
17	*Capricornis* + *Naemorhedus* + *Ovibos*	5.090; 3.089 - 7.588	5.090; 3.089 - 7.588
18	Caprini	9; *7 - 11*	9; *7 - 11*
19	Caprini + *Pantholops*	NE	NE

The intervals in italics are hard uniform calibration bounds, not 95% CIs. NE: not estimated by RelTime.

Declaration of interest

None.

Acknowledgments

The costs associated with the sampling were supported by the private resources of Louiza Derouiche. Carlos Fernandes acknowledges support from Fundação para a Ciência e a Tecnologia (FCT, MCTES, Portugal) and Faculdade de Ciências da Universidade de Lisboa (FCUL) through, respectively, a research grant within the project UID/BIA/00329/2019 and a contract as Invited Assistant Professor (F41699). This work was supported by Portuguese National Funds through FCT in the strategic projects granted to CE3C (grant numbers UID/BIA/00329/2013 and UIDB/00329/2020). We thank three anonymous reviewers and J. Mullins Andrade for their comments and suggestions that helped to improve previous versions of the manuscript.

References

Acevedo, P., Cassinello, J., Hortal, J., Gortázar, C., 2007. Invasive exotic aoudad (*Ammotragus lervia*) as a major threat to native Iberian ibex (*Capra pyrenaica*): a habitat suitability model approach. Divers. Distrib. 13, 587–597.

Adega, F., Silva, R. M., Kjöllerström, H. J., Vercammen, P., Raudsepp, T., Collares-Pereira, M. J., Fernandes, C., Oom M. M., Chaves, R., 2018. Comparative chromosome painting in genets (Carnivora, Viverridae, *Genetta*), the only known feliforms with a highly rearranged karyotype. Cytogenet Genome Res. 156, 35–44.

Akaike, H., 1974. A new look at the statistical model identification. IEEE Trans. Automat. Contr. 19, 716–723.

Alcalá, L., Morales, J., 1997. A primitive caprine from the Upper Vallesian of La Roma 2 (Alfambra, Teruel, Aragón, Spain). C. R. Acad. Sci. IIA. 324, 947–953.

Allen, G. M., 1939. A checklist of African mammals. Bulletin of the Museum of Comparative Zoology 83, 1-763.

Andersen, J. J., Light, J. E., 2012. Phylogeography and subspecies revision of the hispid pocket mouse, *Chaetodipus hispidus* (Rodentia: Heteromyidae). J. Mammal. 93, 1195–1215.

Ashkenazy, H., Penn, O., Doron-Faigenboim, A., Cohen, O., Cannarozzi, G., Zomer, O., Pupko, T., 2012. FastML: a web server for probabilistic reconstruction of ancestral sequences. Nucleic Acids Res. 40, 580–584.

Attard, C. R. M., Möller, L. M., Sasaki M., Hammer, M. P., Bice, C. M., Brauer, C. J., Carvalho, D. C., Harris, J. O., Beheregaray, L. B., 2016. A novel holistic framework for genetic-based captive-breeding and reintroduction programs. Conserv. Biol. 30, 1060-1069.

Avise, J. C., 1989. A role for molecular genetics in the recognition and conservation of endangered species. Trends Ecol. Evol. 4, 279–281.

Avise, J. C., 1995. Mitochondrial DNA polymorphism and a connection between genetics and demography of relevance to conservation. Conserv. Biol. 9, 686–690.

Avise, J. C., Arnold, J., Ball, R. M., Bermingham, E., Lamb, T., Neigel, J. E., Reeb, C. A., Saunders, N. C., 1987. Intraspecific phylogeography: the mitochondrial DNA bridge between population genetics and systematics. Ann. Rev. Ecol. Syst. 18, 489–522.

Avise, J. C., Ball, R. M., 1990. Principles of genealogical concordance in species concepts and biological taxonomy. Oxf. Surv. Evol. Biol. 7, 45–67.

Avise, J. C., Ball, R. M., Arnold, J., 1988. Current versus historical population sizes in vertebrate species with high gene flow: a comparison based on mitochondrial DNA lineages and inbreeding theory for neutral mutations. Mol. Biol. Evol. 5, 331–344.

Bandelt, H-J., Forster, P., Rohl, A., 1999. Median-joining networks for inferring intraspecific phylogenies. Mol. Biol. Evol. 16, 37–48.

Barba-Montoya, J., dos Reis, M., Yang, Z., 2017. Comparison of different strategies for using fossil calibrations to generate the time prior in Bayesian molecular clock dating. Mol. Phylogenet. Evol. 114, 386–400.

Barrowclough, G. F., Zink, R. M., 2009. Funds enough, and time: mtDNA, nuDNA and the discovery of divergence. Mol. Ecol. 18, 2934-2936.

Battistuzzi, F. U., Filipski, A., Hedges, S. B., Kumar, S., 2010. Performance of relaxed-clock methods in estimating evolutionary divergence times and their credibility intervals. Mol. Biol. Evol. 27, 1289–1300.

Battistuzzi, F. U., Tao, Q., Jones, L., Tamura, K., Kumar, S., 2018. RelTime relaxes the strict molecular clock throughout the phylogeny. Genome Biol. Evol. 10, 1631–1636.

Bensasson, D., Zhang, D-X., Hartl, D. L., Hewitt, G. M., 2001. Mitochondrial pseudogenes: evolution's misplaced witnesses. Trends Ecol. Evol. 16, 314-321.

Berry, V., Gascuel, O., 1996. On the interpretation of bootstrap trees: appropriate threshold of clade selection and induced gain. Mol. Biol. Evol. 13, 999–1011.

Bibi, F., 2013. A multi-calibrated mitochondrial phylogeny of extant Bovidae (Artiodactyla, Ruminantia) and the importance of the fossil record to systematics. BMC Evol. Biol. 13, 166.

Björklund, M., 2003. Test for a population expansion after a drastic reduction in population size using DNA sequence data. Heredity 91, 481–486.

Bollback, J. P., 2006. SIMMAP: stochastic character mapping of discrete traits on phylogenies. BMC Bioinformatics 7, 88.

Bounaceur, F., Benamor, N., Bissaad, F. Z., Abdi, A., Aulagnier, S., 2016. Is there a future for the last populations of aoudad (*Ammotragus lervia*) in northern Algeria?. Pakistan J. Zool. 48, 1727–1731.

Bradley, R. D., Baker, R. J., 2001. A test of the genetic species concept: cytochrome-b sequences and mammals. J. Mammal. 82, 960–973.

Bromham, L., Duchêne, S., Hua, X., Ritchie, A. M., Duchêne, D. A., Ho, S. Y. W., 2018. Bayesian molecular dating: opening up the black box. Biol. Rev. 93, 1165–1191.

Brown, J. W., Smith, S. A., 2018. The past sure is tense: on interpreting phylogenetic divergence time estimates. Syst. Biol. 67, 340–353.

Brown, R. P., Yang, Z., 2011. Rate variation and estimation of divergence times using strict and relaxed clocks. BMC Evol. Biol. 11, 271.

Brown, W. M., George Jr, M., Wilson, A. C., 1979. Rapid evolution of animal mitochondrial DNA. Proc. Natl. Acad. Sci. U.S.A. 76, 1967–1971.

Buchalski, M. R., Sacks, B. N., Gille, D. A., Penedo, M. C. T., Ernest, H. B., Morrison, S. A., Boyce, W. M., 2016. Phylogeographic and population genetic structure of bighorn sheep (*Ovis canadensis*) in North American deserts. J. Mammal. 97, 823–838.

Bunch, T. D. Wu, C., Zhang, Y.-P., Wang, S., 2006. Phylogenetic analysis of snow sheep (*Ovis nivicola*) and closely related taxa. J. Hered. 97, 21–30.

Cassens, I., Van Waerebeek, K., Best, P. B., Crespo, E. A., Reyes, J., Milinkovitch, M. C., 2003. The phylogeography of dusky dolphins (*Lagenorhynchus obscurus*): a critical examination of network methods and rooting procedures. Mol. Ecol. 12, 1781–1792.

Cassinello, J., 1998. *Ammotragus lervia*: a review on systematics, biology, ecology and distribution. Ann. Zool. Fennici 35, 149–162.

Cassinello, J., Serrano, E., Calabuig, G., Perez, J. M., 2004. Range expansion of an exotic ungulate (*Ammotragus lervia*) in southern Spain: ecological and conservation concerns. Biodivers. Conserv. 13, 851–866.

Cassinello, J., Cuzin, F., Jdeidi, T., Masseti, M., Nader, I., De Smet, K., 2008. *Ammotragus lervia*. The IUCN Red List of Threatened Species. http://dx.doi.org/10.2305/IUCN.UK.2008.RLTS.T1151A3288917.en

Charruau, P., Fernandes, C., Orozco-terWengel, P., Peters, J., Hunter, L., Ziaie, H., Jourabchian, A., Jowkar, H., Schaller, G., Ostrowski, S., Vercammen, P., Grange, T., Schlotterer, C., Kotze, A., Geigl, E. M., Walzer, C., Burger, P. A., 2011. Phylogeography, genetic structure and population divergence time of cheetahs in Africa and Asia: evidence for long-term geographic isolates. Mol. Ecol. 20, 706–724.

Clement, M., Posada, D., Crandall, K. A., 2000. TCS: a computer program to estimate gene genealogies. Mol. Ecol. 9, 1657-1659.

Curtain, C. C., Fudenberg, H. H., 1973. Evolution of the immunoglobulin antigens in the Ruminantia. Biochem. Genet. 8, 301-308.

Cuzin, F., 1996. Répartition actuelle et statut des grands mammifères sauvages du Maroc (Primates, Carnivores, Artiodactyles). Mammalia 60, 101–124.

Darriba, D., Taboada, G. L., Doallo, R., Posada, D., 2012. jModelTest 2: more models, new heuristics and parallel computing. Nat. Methods 9, 772.

De Smet, K., 1997. Algeria. In: Shackleton, D. M. (Ed.), IUCN/SSC Caprinae Specialist Group. Wild sheep and goats and their relatives: status survey and conservation action plan for Caprinae. I.U.C.N., Gland, Switzerland and Cambridge, UK, pp. 17–19.

Derouiche, L., Vercammen, P., Bouhadad, R., Fernandes, C. 2017. Genetic evidence supporting the taxonomic separation of the Arabian and Northwest African subspecies of the desert hedgehog (*Paraechinus aethiopicus*). Gene 620, 54-65.

Dornburg, A., Brandley, M. C., McGowen, M. R., Near, T. J., 2012. Relaxed clocks and inferences of heterogeneous patterns of nucleotide substitution and divergence time estimates across whales and dolphins (Mammalia: Cetacea). Mol. Biol. Evol. 29, 721–736.

Dotsev, A. V., Deniskova, T. E., Okhlopkov, I. M., Mészáros, G., Sölkner, J., Reyer, H., Wimmers, K., Brem, G., Zinovieva, N. A., 2018. Genome-wide SNP analysis unveils genetic structure and phylogeographic history of snow sheep (*Ovis nivicola*) populations inhabiting the Verkhoyansk Mountains and Momsky Ridge (northeastern Siberia). Ecol. Evol. 8, 8000–8010.

Drummond, A. J., Ho, S. Y. W., Phillips, M. J. Rambaut, A., 2006. Relaxed phylogenetics and dating with confidence. PLoS Biol. 4, e88.

Drummond, A. J., Suchard, M. A., Xie, D., Rambaut, A., 2012. Bayesian phylogenetics with BEAUti and the BEAST 1.7. Mol. Biol. Evol. 29, 1969–1973.

Dubach, J. M., Briggs, M. B., White, P. A., Ament, B. A., Patterson, B. D., 2013. Genetic perspectives on ‘‘lion conservation units’’ in Eastern and Southern Africa. Conserv. Genet. 14, 741–755.

Duchêne, S., Lanfear, R., Ho, S. Y. W., 2014. The impact of calibration and clock-model choice on molecular estimates of divergence times. Mol. Phylogenet. Evol. 78, 277–289.

Eizirik, E., Kim, J. H., Menotti-Raymond, M., Crawshaw Jr, P. G., O’Brien, S. J., Johnson, W. E., 2001. Phylogeography, population history and conservation genetics of jaguars (*Panthera onca*, Mammalia, Felidae). Mol. Ecol. 10, 65–79.

Evin, A., Baylac, M., Ruedi, M., Mucedda, M., Pons, J. M., 2008. Taxonomy, skull diversity and evolution in a species complex of *Myotis* (Chiroptera: Vespertilionidae): a geometric morphometric appraisal. Biol. J. Linn. Soc. 95, 529–538.

Excoffier, L., Lischer, H. E. L., 2010. Arlequin suite ver 3.5: a new series of programs to perform population genetics analyses under Linux and Windows. Mol. Ecol. Resour. 10, 564–567.

Felsenstein, J., 1985. Confidence limits on phylogenies: an approach using the bootstrap. Evolution 39, 783–791.

Fernandes, C. A., Ginja, C., Pereira, I., Tenreiro, R., Bruford, M. W., Santos-Reis, M., 2008. Species-specific mitochondrial DNA markers for identification of non-invasive samples from sympatric carnivores in the Iberian Peninsula. Conserv. Genet. 9, 681–690.

Fraser, D. J., Bernatchez, L., 2001. Adaptive evolutionary conservation: towards a unified concept for defining conservation units. Mol. Ecol. 10, 2741-2752.

Fu, Y-X., 1997. Statistical tests of neutrality of mutations against population growth, hitchhiking and background selection. Genetics 147, 915–925.

Fu, Y-X., Li, W-H., 1999. Coalescing into the 21st century: an overview and prospects of coalescent theory. Theor. Popul. Biol. 56, 1–10.

Gaggiotti, O. E., Excoffier, L., 2000. A simple method of removing the effect of a bottleneck and unequal population sizes on pairwise genetic distances. Proc. R. Soc. Lond. B. 267, 81-87.

Gernhard, T., 2008. The conditioned reconstructed process. J. Theor. Biol. 253, 769–778.

Glez-Peña, D., Gómez-Blanco, D., Reboiro-Jato, M., Fdez-Riverola, F., Posada, D., 2010. ALTER: program-oriented conversion of DNA and protein alignments. Nucleic Acids Res. 38, 14–18.

Grant, W. A. S., Bowen, B. W., 1998. Shallow population histories in deep evolutionary lineages of marine fishes: insights from sardines and anchovies and lessons for conservation. J. Hered. 89, 415–426.

Gray, G. G., Simpson, C. D., 1980. *Ammotragus lervia*. Mamm. Species. 144, 1–7.

Grubb, P., 2005. Order Artiodactyla. In Wilson, D. E., Reeder, D. M. (Eds.), Mammal Species of the World. A Taxonomic and Geographic Reference, third ed. vol. 1. The Johns Hopkins University Press. Baltimore, pp. 637–722.

Guindon, S., Dufayard, J-F., Lefort, V., Anisimova, M., Hordijk, W., Gascuel, O., 2010. New algorithms and methods to estimate maximum-likelihood phylogenies: assessing the performance of PhyML 3.0. Syst. Biol. 59, 307–321.

Hanke, M., Wink, M., 1994. Direct DNA sequencing of PCR-amplified vector inserts following enzymatic degradation of primer and dNTPs. Biotechniques 17, 858–860.

Harpending, H. C., 1994. Signature of ancient population growth in a low-resolution mitochondrial DNA mismatch distribution. Hum. Biol. 66, 591–600.

Harper, F., 1940. The nomenclature and type localities of certain Old World mammals. J. Mammal. 21, 191-203.

Harris, R. B., 2014. *Pseudois nayaur*. The IUCN Red List of Threatened Species. http://dx.doi.org/10.2305/IUCN.UK.2014-3.RLTS.T61513537A64313015.en.

Harrison, R. G., 1989. Animal mitochondrial DNA as a genetic marker in population and evolutionary biology. Trends Ecol. Evol. 4, 6–11.

Hart, M. W., Sunday, J, 2007. Things fall apart: biological species form unconnected parsimony networks. Biol. Lett. 3, 509-512.

Hasegawa, M., Kishino, H., Yano, T. A., 1985. Dating of the human-ape splitting by a molecular clock of mitochondrial DNA. J. Mol. Evol. 22, 160–174.

Hassanin, A., Douzery, E. J. P., 1999. The tribal radiation of the family Bovidae (Artiodactyla) and the evolution of the mitochondrial cytochrome *b* gene. Mol. Phylogenet. Evol. 13, 227–243.

Hassanin, A., Ropiquet, A., 2007. Resolving a zoological mystery: the kouprey is a real species. Proc. R. Soc. Lond. B. 274, 2849–2855.

Hassanin, A., Delsuc, F., Ropiquet, A., Hammer, C., van Vuuren, B. J., Matthee, C., Ruiz-Garcia, M., Catzeflis, F., Areskoug, V., Nguyen, T. T., Couloux, A., 2012. Pattern and timing of diversification of Cetartiodactyla (Mammalia, Laurasiatheria), as revealed by a comprehensive analysis of mitochondrial genomes. C. R. Biol. 335, 32–50.

Hassanin, A., Pasquet, E., Vigne, J-D., 1998. Molecular systematics of the subfamily Caprinae (Artiodactyla, Bovidae) as determined from cytochrome *b* sequences. J. Mamm. Evol. 5, 217-236.

Hassanin, A., Ropiquet, A., Couloux, A., Cruaud, C., 2009. Evolution of the mitochondrial genome in mammals living at high altitude: new insights from a study of the tribe Caprini (Bovidae, Antilopinae). J. Mol. Evol. 68, 293–310.

Hedrick, P. W., 1999. Perspective: highly variable loci and their interpretation in evolution and conservation. Evolution 53, 313–318.

Heled, J., Bouckaert, R. R., 2013. Looking for trees in the forest: summary tree from posterior samples. BMC Evol. Biol. 13, 221.

Heled, J., Drummond, A. J., 2012. Calibrated tree priors for relaxed phylogenetics and divergence time estimation. Syst. Biol. 61, 138–149.

Hey, J., 2005. On the number of New World founders: a population genetic portrait of the peopling of the Americas. PLoS Biol. 3, e193.

Hey, J., Nielsen, R., 2004. Multilocus methods for estimating population sizes, migration rates and divergence time, with applications to the divergence of *Drosophila pseudoobscura* and *D. persimilis*. Genetics 167, 747–760.

Hey, J., Nielsen, R., 2007. Integration within the Felsenstein equation for improved Markov chain Monte Carlo methods in population genetics. Proc. Natl. Acad. Sci. U.S.A. 104, 2785–2790.

Hight, M. E., Nadler, C. F., 1976. Relationships Between wild sheep and goats and the aoudad (Caprini) studied by immunodiffusion. Comp. Biochem. Phys. B. 54, 265–269.

Ho, S. Y. W., Duchêne, S., Duchêne, D., 2015. Simulating and detecting autocorrelation of molecular evolutionary rates among lineages. Mol. Ecol. Resour. 15, 688–696.

Ho, S. Y. W., Lanfear, R., Bromham, L., Phillips, M. J., Soubrier, J., Rodrigo, A. G., Cooper, A., 2011. Time-dependent rates of molecular evolution. Mol. Ecol. 20, 3087–3101.

Ho, S. Y. W., Phillips, M. J., Drummond, A. J., Cooper A., 2005a. Accuracy of rate estimation using relaxed-clock models with a critical focus on the early metazoan radiation. Mol. Biol. Evol. 22, 1355–1363.

Ho, S. Y. W., Phillips, M. J., Cooper A., Drummond, A. J., 2005b. Time dependency of molecular rate estimates and systematic overestimation of recent divergence times. Mol. Biol. Evol. 22, 1561–1568.

Ho, S. Y. W., Shapiro, B., Phillips, M. J., Cooper, A., Drummond, A. J., 2007. Evidence for time dependency of molecular rate estimates. Syst. Biol. 56, 515–522.

Holder, M. T., Sukumaran, J., Lewis, P. O., 2008. A justification for reporting the majority-rule consensus tree in Bayesian phylogenetics. Syst. Biol. 57, 814–821.

Hopwood, A. T., Hollyfield, J. P., 1954. An annotated bibliography of the fossil mammals of Africa (1742-1950). Fossil Mammals of Africa No. 8. British Museum (Natural History), London.

Huelsenbeck, J. P., Larget, B., Alfaro, M. E., 2004. Bayesian phylogenetic model selection using reversible jump Markov chain Monte Carlo. Mol. Biol. Evol. 21, 1123–1133.

Huggins, P. M., Li, W., Haws, D., Friedrich, T., Liu, J., Yoshida, R., 2011. Bayes estimators for phylogenetic reconstruction. Syst. Biol. 60, 528–540.

Hurvich, C. M., Tsai, C-L., 1989. Regression and time series model selection in small samples. Biometrika 76, 297–307.

Irwin, D. M., Kocher, T. D., Wilson, A. C., 1991. Evolution of the cytochrome *b* gene of mammals. J. Mol. Evol. 32, 128–144.

Jansen, T., Forster, P., Levine, M. A., Oelke, H., Hurles, M., Renfrew, C., Weber, J., Olek, K., 2002. Mitochondrial DNA and the origins of the domestic horse. Proc. Natl. Acad. Sci. U.S.A. 99, 10905-10910.

Jiang, L., Wang, G., Tan, S., Gong, S., Yang, M., Peng, Q., Peng, R., Zou, F., 2013. The complete mitochondrial genome sequence analysis of Tibetan argali (*Ovis ammon hodgsoni*): Implications of Tibetan argali and Gansu argali as the same subspecies. Gene 521, 24–31.

Jiang, Y., Xie, M., Chen, W., Talbot, R., Maddox, J. F., Faraut, T., Wu, C., Muzny, D. M., Li, Y., Zhang, W., Stanton, J-A., Brauning, R., Barris, W. C., Hourlier, T., Aken, B. L., Searle, S. M. J., Adelson, D. L., Bian, C., Cam, G. R., Chen, Y., Cheng, S., DeSilva, U., Dixen, K., Dong, Y., Fan, G., Franklin, I. R., Fu, S., Fuentes-Utrilla, P., Guan, R., Highland, M. A., Holder, M. E., Huang, G., Ingham, A. B., Jhangiani, S. N., Kalra, D., Kovar, C. L., Lee, S. L., Liu, W., Liu, X., Lu, C., Lv, T., Mathew, T., McWilliam, S., Menzies, M., Pan, S., Robelin, D., Servin, B., Townley, D.,

Wang, W., Wei, B., White, S. N., Yang, X., Ye, C., Yue, Y., Zeng, P., Zhou, Q., Hansen, J. B., Kristiansen, K., Gibbs, R. A., Flicek, P., Warkup, C. C., Jones, H. E., Oddy, V. H., Nicholas, F. W., McEwan, J. C., Kijas, J. W., Wang, J., Worley, K. C., Archibald, A. L., Cockett, N., Xu, X., Wang, W., Dalrymple, B. P., 2014. The sheep genome illuminates biology of the rumen and lipid metabolism. Science 344, 1168-1173.

Johns, G. C., Avise, J. C., 1998. A comparative summary of genetic distances in the vertebrates from the mitochondrial cytochrome *b* gene. Mol. Biol. Evol. 15, 1481–1490.

Kent, W. J., Sugnet, C. W., Furey, T. S., Roskin, K. M., Pringle, T. H., Zahler, A. M., Haussler, D., 2002. The human genome browser at UCSC. Genome Res. 12, 996–1006.

Kimura, M., 1980. A simple method for estimating evolutionary rates of base substitutions through comparative studies of nucleotide sequences. J. Mol. Evol. 16, 111–120.

Kingdon, J., 1982. East African Mammals: An Atlas of Evolution in Africa, Volume IIID Bovids. The University of Chicago Press, Chicago.

Kingdon, J., 1997. The Kingdon Field Guide to African Mammals. Academic Press, London.

Kingdon J., Hoffmann, M. (Eds.), 2013. Mammals of Africa. Volume VI. Bloomsbury Publishing, London.

Kowalski, K., Rzebik-Kowalska, B., 1991. Mammals of Algeria. Polish Academy of Science, Institute of Systematics and Evolution of Animals, Wroclaw.

Kumar, S., Hedges, S. B., 2016. Advances in time estimation methods for molecular data. Mol. Biol. Evol. 33, 863–869.

Kumar, S., Stecher, G., Li, M., Knyaz, C., Tamura, K., 2018. MEGA X: molecular evolutionary genetics analysis across computing platforms. Mol. Biol. Evol. 35, 1547–1549.

Kumar, S., Stecher, G., Tamura, K., 2016. MEGA7: Molecular Evolutionary Genetics Analysis Version 7.0 for bigger datasets. Mol. Biol. Evol. 33, 1870–1874.

Lalueza-Fox, C., Castresana, J., Sampietro, L., Marquès-Bonet, T., Alcover, J. A., Bertranpetit, J., 2005. Molecular dating of caprines using ancient DNA sequences of *Myotragus balearicus*, an extinct endemic Balearic mammal. BMC Evol. Biol. 5, 70.

Lanave, C., Preparata, G., Saccone, C., Serio, G., 1984. A new method for calculating evolutionary substitution rates. J. Mol. Evol. 20, 86–93.

Lanfear, R., Frandsen, P. B., Wright, A. M., Senfeld, T., Calcott, B., 2016. PartitionFinder 2: New methods for selecting partitioned models of evolution for molecular and morphological phylogenetic analyses. Mol. Biol. Evol. 34, 772-773.

Larrasoaña, J. C., Roberts, A. P., Rohling, E. J., 2013. Dynamics of green Sahara periods and their role in hominin evolution. PloS ONE 8, e76514.

Leigh, J. W., Bryant, D., 2015. POPART: full-feature software for haplotype network construction. Methods Ecol. Evol. 6, 1110–1116.

Lepage, T., Bryant, D., Philippe, H., Lartillot, N., 2007. A general comparison of relaxed molecular clock models. Mol. Biol. Evol. 24, 2669–2680.

Lerp, H., Wronski, T., Pfenninger, M., Plath, M., 2011. A phylogeographic framework for the conservation of Saharan and Arabian Dorcas gazelles (Artiodactyla: Bovidae). Org. Divers. Evol. 11, 317.

Librado, P., Rozas, J., 2009. DnaSP v5: a software for comprehensive analysis of DNA polymorphism data. Bioinformatics 25, 1451–1452.

Loggers, C. O., Thévenot, M., Aulagnier, S., 1992. Status and distribution of Moroccan wild ungulates. Biol. Conserv. 59, 9–18.

Ludwig, A., Fischer, S., 1998. New aspects of an old discussion - phylogenetic relationships of *Ammatragus* and *Pseudois* within the subfamily Caprinae based on comparison of the 12s rDNA sequences. J. Zool. Syst. Evol. Res. 36, 173–178.

Lynch, M., Pfrender, M., Spitze, K., Lehman, N., Hicks, J., Allen, D., Latta, L., Ottene M., Bogue, F., Colbourne, J., 1999. The quantitative and molecular genetic architecture of a subdivided species. Evolution 53, 100–110.

Manceau, V., Crampe, J. P., Boursot, P., Taberlet, P., 1999. Identification of evolutionary significant units in the Spanish wild goat, *Capra pyrenaica* (Mammalia, Artiodactyla). Anim. Conserv. 2, 33–39.

Manlius, N., Menardi-Noguera, A., Zboray, A., 2003. Decline of the Barbary sheep (*Ammotragus lervia*) in Egypt during the 20th century: literature review and recent observations. J. Zool. 259, 403–409.

Manwell, C., Ann Baker, C. M., 1975. *Ammotragus lervia*: progenitor of the domesticated sheep or specialized offshoot of caprine evolution?. Experientia 31, 1370-1371.

Manwell, C., Ann Baker, C. M., 1977. *Ammotragus lervia*: Barbary sheep or Barbary goat?. Comp. Biochem. Phys. B 58, 267–271.

Maruyama, T., Fuerst, P. A., 1984. Population bottlenecks and nonequilibrium models in population genetics. I. allele numbers when populations evolve from zero variability. Genetics 108, 745-763.

Maruyama, T., Fuerst, P. A., 1985. Population bottlenecks and nonequilibrium models in population genetics. II. number of alleles in a small population that was formed by a recent bottleneck. Genetics 111, 675–689.

Matthee, C. A., Davis, S. K., 2001. Molecular insights into the evolution of the family Bovidae: a nuclear DNA perspective. Mol. Biol. Evol. 18, 1220-1230.

Mead, J. I., Taylor, L. H., 2005. New species of *Sinocapra* (Bovidae, Caprinae) from the lower Pliocene Panaca Formation, Nevada, USA. Palaeontol. Electron. 8, 11A.

Mello, B., Tao, Q., Tamura, K., Kumar, S., 2017. Fast and accurate estimates of divergence times from big data. Mol. Biol. Evol. 34, 45–50.

Mereu, P., di Suni, M. P., Manca, L., Masala, B., 2008. Complete nucleotide mtDNA sequence of Barbary sheep (*Ammotragus lervia*). DNA Sequence 19, 241–245.

Merilä, J., Crnokrak, P., 2001. Comparison of genetic differentiation at marker loci and quantitative traits. J. Evol. Biol. 14, 892–903.

Mimoun, J. B., Cassinello, J., Nouira, S., 2017. Update of the distribution and status of the aoudad *Ammotragus lervia* (Bovidae, Caprini) in Tunisia. Mammalia 81, 181-187.

Moore, W. S., 1995. Inferring phylogenies from mtDNA variation: mitochondrial-gene trees versus nuclear-gene trees. Evolution 49, 718–726.

Moritz, C., 1994. Defining 'Evolutionarily Significant Units' for conservation. Trends Ecol. Evol. 9, 373–375.

Moritz, C., Dowling, T. E., Brown, W. M., 1987. Evolution of animal mitochondrial DNA: relevance for population biology and systematics. Ann. Rev. Ecol. Syst. 18, 269–292.

Moritz, C., 2002. Strategies to protect biological diversity and the evolutionary processes that sustain it. Syst. Biol. 51, 238–254.

Mulcahy, D. G., 2008. Phylogeography and species boundaries of the western North American Night snake (*Hypsiglena torquata*): Revisiting the subspecies concept. Mol. Phylogenet. Evol. 46, 1095–1115.

Nei, M., 1987. Molecular Evolutionary Genetics. Columbia University Press, New York.

Nei, M., Li, W. H., 1979. Mathematical model for studying genetic variation in terms of restriction endonucleases. Proc. Natl. Acad. Sci. U.S.A. 76, 5269–5273.

Neigel, J. E., Avise, J. C., 1993. Application of a random walk model to geographic distributions of animal mitochondrial DNA variation. Genetics 135, 1209–1220.

Nogales, M., Rodríguez-Luengo, J. L., Marrero, P., 2006. Ecological effects and distribution of invasive non-native mammals on the Canary Islands. Mammal Rev. 36, 49–65.

O'Brien, S. J., Mayr, E., 1991. Bureaucratic mischief: recognizing endangered species and subspecies. Science 251, 1187–1188.

Peng, Q., Tang, L., Tan, S., Li, Z., Wang, J., Zou, F., 2012. Mitogenomic analysis of the genus *Pseudois*: evidence of adaptive evolution of morphological variation in the ATP synthase genes. Mitochondrion 12, 500–505.

Pérez, T., González, I., Essler, S. E., Fernández, M., Domínguez, A., 2014. The shared mitochondrial genome of *Rupicapra pyrenaica ornata* and *Rupicapra rupicapra cartusiana*: old remains of a common past. Mol. Phylogenet. Evol. 79, 375–379.

Pérez, T., Rodríguez, F., Fernández, M., Albornoz, J., Domínguez, A., 2017. Ancient mitochondrial pseudogenes reveal hybridization between distant lineages in the evolution of the *Rupicapra* genus. Gene 628, 63–71.

Pesole, G., Gissi, C., De Chirico, A., Saccone, C., 1999. Nucleotide substitution rate of mammalian mitochondrial genomes. J. Mol. Evol. 48, 427–434.

Pirastru, M., Multineddu, C., Mereu, P., Sannai, M., El Sherbini, E. S., Hadjisterkotis, E., Nàhlik, A., Franceschi, P., Manca, L., Masala, B., 2009. The sequence and phylogenesis of the α-globin genes of Barbary sheep (*Ammotragus lervia*), goat (*Capra hircus*), European

mouflon (*Ovis aries musimon*) and Cyprus mouflon (*Ovis aries ophion*). Comp. Biochem. Phys. D 4, 168–173.

Prieto-Torres, D. A., Cuervo, A. M., Bonaccorso, E. 2018. On geographic barriers and Pleistocene glaciations: tracing the diversification of the russet-crowned warbler (*Myiothlypis coronata*) along the Andes. PloS ONE, 13, e0191598.

Rambau, R. V., Robinson, T. J., Stanyon, R., 2003. Molecular genetics of *Rhabdomys pumilio* subspecies boundaries: mtDNA phylogeography and karyotypic analysis by fluorescence in situ hybridization. Mol. Phylogenet. Evol. 28, 564–575.

Rambaut, A., Drummond, A. J., Xie, D., Baele, G., Suchard, M. A., 2018. Posterior summarization in Bayesian phylogenetics using Tracer 1.7. Syst. Biol. 67, 901–904.

Ramos-Onsins S. E., Rozas, J., 2002. Statistical properties of new neutrality tests against population growth. Mol. Bio. Evol. 19, 2092–2100.

Rebholz, W., Harley, E., 1999. Phylogenetic relationships in the bovid subfamily Antilopinae based on mitochondrial DNA sequences. Mol. Phylogenet. Evol. 12, 87–94.

Rezaei, H. R., Naderi, S., Chintauan-Marquier, I., Taberlet, P., Virk, A., Naghash, H., Rioux, D., Kaboli, M., Pompanon, F., 2010. Evolution and taxonomy of the wild species of the genus *Ovis* (Mammalia, Artiodactyla, Bovidae). Mol. Phylogenet. Evol. 54, 315–326.

Rogers, A. R., Harpending, H., 1992. Population growth makes waves in the distribution of pairwise genetic differences. Mol. Biol. Evol. 9, 552–569.

Rohling, E. J., Marino, G., Grant, K. M., 2015. Mediterranean climate and oceanography, and the periodic development of anoxic events (sapropels). Earth-Sci. Rev. 143, 62–97.

Romer, A. S., 1928. Pleistocene mammals of Algeria: fauna of the Paleolithic station of Mechta-el-Arbi. Logan. Mus. Bull. 1, 80–163.

Ronquist, F., Teslenko, M., van der Mark, P., Ayres, D. L., Darling, A., Höhna, S., Larget, B., Liu, L., Suchard, M. A., Huelsenbeck, J. P., 2012. MrBayes 3.2: Efficient Bayesian phylogenetic inference and model choice across a large model space. Syst. Biol. 61, 539–542.

Ropiquet, A., Hassanin, A., 2005a. Molecular evidence for the polyphyly of the genus *Hemitragus* (Mammalia, Bovidae). Mol. Phylogenet. Evol. 36, 154–168.

Ropiquet, A., Hassanin, A., 2005b. Molecular phylogeny of caprines (Bovidae, Antilopinae): the question of their origin and diversification during the Miocene. J. Zool. Syst. Evol. Res. 43, 49–60.

Ropiquet, A., Hassanin, A., 2006. Hybrid origin of the Pliocene ancestor of wild goats. Mol. Phylogenet. Evol. 41, 395–404.

Rothschild, W., 1913. On *Ovis lervia* Pallas and its subspecies. Novit. Zool. 20, 459–460.

Rothschild, W., 1921. Captain Angus Buchanan's Air expedition. III. Ungulate mammals collected by Captain Angus Buchanan. Novit. Zool. 28, 75-77.

Ryder, O. A., 1986. Species conservation and systematics: the dilemma of subspecies. Trends Ecol. Evol. 1, 9–10.

Sanna, D., Barbato, M., Hadjisterkotis, E., Cossu, P., Decandia, L., Trova, S., Pirastru, M., Leoni, G. G., Naitana, S., Francalacci, P., Masala, B., Manca, L., Mereu, P., 2015. The first mitogenome of the Cyprus mouflon (*Ovis gmelini ophion*): new insights into the phylogeny of the genus *Ovis*. PLoS ONE 10, 0144257.

Sano, A., Tachida, H., 2005. Gene genealogy and properties of test statistics of neutrality under population growth. Genetics 169, 1687-1697.

Schlieben, S., Erhardt, G., Senft, B., 1991. Genotyping of bovine k-casein (k-CN^{A}, k- CN^{B}, k-CN^{C}, k-CN^{E}) following DNA sequence amplification and direct sequencing of k-CN^{E} PCR product. Anim. Genet. 22, 333–342.

Schwarz G., 1978. Estimating the dimension of a model. Ann. Stat. 6, 461–464.

Shackleton, D. M. (Ed.), IUCN/SSC Caprinae Specialist Group, 1997. Wild sheep and goats and their relatives: status survey and conservation action plan for Caprinae. I.U.C.N., Gland, Switzerland and Cambridge, UK.

Silva, T. L., Godinho, R., Castro, D., Abáigar, T., Brito, J. C., Alves, P. C., 2015. Genetic identification of endangered North African ungulates using noninvasive sampling. Mol. Ecol. Resour. 15, 652–661.

Silva, T. L., Vale, C. G., Godinho, R., Fellous, A., Hingrat, Y., Alves, P. C., Abáigar, T., Brito, J. C., 2017. Ecotypes and evolutionary significant units in endangered North African gazelles. Biol. J. Linn. Soc. 122, 286–300.

Sim, Z., Hall, J. C., Jex, B., Hegel, T. M., Coltman, D. W., 2016. Genome-wide set of SNPs reveals evidence for two glacial refugia and admixture from postglacial recolonization in an alpine ungulate. Mol. Ecol. 25, 3696–3705.

Simonsen, K. L., Churchill, G. A., Aquadro, C. F., 1995. Properties of statistical tests of neutrality for DNA polymorphism data. Genetics 141, 413–429.

Stamatakis, A., 2014. RAxML version 8: a tool for phylogenetic analysis and post-analysis of large phylogenies. Bioinformatics 30, 1312–1313.

Sugiura, N., 1978. Further analysts of the data by akaike's information criterion and the finite corrections. Commun. Stat. Theo. Meth. 7, 13–26.

Sukumaran, J., Holder, M. T., 2010. DendroPy: a Python library for phylogenetic computing. Bioinformatics 26, 1569–1571.

Tajima, F., 1989a. Statistical method for testing the neutral mutation hypothesis by DNA polymorphism. Genetics 123, 585–595.

Tajima, F., 1989b. The effect of change in population size on DNA polymorphism. Genetics 123, 597–601.

Tajima, F., 1993. Simple methods for testing the molecular evolutionary clock hypothesis. Genetics 135, 599–607.

Takezaki, N., Nei, M., 1996. Genetic distances and reconstruction of phylogenetic trees from microsatellite DNA. Genetics 144, 389–399.

Tamura, K., Kumar, S., 2002. Evolutionary distance estimation under heterogeneous substitution pattern among lineages. Mol. Biol. Evol. 19, 1727–1736.

Tamura, K., Nei, M., 1993. Estimation of the number of nucleotide substitutions in the control region of mitochondrial DNA in humans and chimpanzees. Mol. Biol. Evol. 10, 512–526.

Tamura, K., Battistuzzi, F. U., Billing-Ross, P., Murillo, O., Filipski, A., Kumar, S., 2012. Estimating divergence times in large molecular phylogenies. Proc. Natl. Acad. Sci. U.S.A. 109, 19333–19338.

Tamura, K., Tao, Q., Kumar, S., 2018. Theoretical foundation of the RelTime method for estimating divergence times from variable evolutionary rates. Mol. Biol. Evol. 35, 1770–1782.

Tao, Q., Tamura, K., Battistuzzi, F. U., Kumar, S., 2019. A machine learning method for detecting autocorrelation of evolutionary rates in large phylogenies. Mol. Biol. Evol. 36, 811–824.

Tchaicka, L., Eizirik, E., De Oliveira, T. G., Candido Jr, J. F., Freitas, T. R., 2007. Phylogeography and population history of the crab-eating fox (*Cerdocyon thous*). Mol. Ecol. 16, 819–838.

Templeton, A. R., Crandall, K. A., & Sing, C. F., 1992. A cladistic analysis of phenotypic associations with haplotypes inferred from restriction endonuclease mapping and DNA sequence data. III. Cladogram estimation. Genetics 132, 619-633.

Templeton, A. R., Routman, E., Phillips, C. A., 1995. Separating population structure from population history: a cladistic analysis of the geographical distribution of mitochondrial DNA haplotypes in the tiger salamander, *Ambystoma tigrinum*. Genetics 140, 767–782.

Thorne, J. L., Kishino, H., Painter, I. S., 1998. Estimating the rate of evolution of the rate of molecular evolution. Mol. Biol. Evol. 15, 1647–1657.

Tyner, C., Barber, G. P., Casper, J., Clawson, H., Diekhans, M., Eisenhart, C., Fischer, C. M., Gibson, D., Gonzalez, J. N., Guruvadoo, L., Haeussler, M., Heitner, S., Hinrichs, A. S., Karolchik, D., Lee, B. T., Lee, C. M., Nejad, P., Raney, B. J., Rosenbloom, K. R, Speir, M. L., Villarreal, C., Vivian, J., Zweig, A. S., Haussler, D., Kuhn, R. M., Kent, W. J., 2017. The UCSC Genome Browser database: 2017 update. Nucleic Acids Res. 45, D626–D634.

Van Dam, J. A., Alcalá, L., Zarza, A. A., Calvo, J. P., Garcés, M., Krijgsman, W., 2001. The upper Miocene mammal record from the Teruel-Alfambra region (Spain). The MN system and continental stage/age concepts discussed. J. Vertebr. Paleontol. 21, 367–385.

Villesen, P., 2007. FaBox: an online toolbox for FASTA sequences. Mol. Ecol. Notes 7, 965–968.

Vogler, A. P., DeSalle, R., 1994. Diagnosing units of conservation management. Conserv. Biol. 8, 354-363.

Werle, E., Schneider, C., Renner, M., Völker, M., Fiehn, W., 1994. Convenient single-step, one tube purification of PCR products for direct sequencing. Nucleic Acids Res. 22, 4354–4355.

Wilson, A. C., Cann, R. L., Carr, S. M., George, M., Gyllensten, U. B., Helm-Bychowski, K. M., Higuchi, R. G., Palumbi, S. R., Prager, E. M., Sage, R. D., Stoneking, M., 1985. Mitochondrial DNA and two perspectives on evolutionary genetics. Biol. J. Linn. Soc. 26, 375–400.

Wyner, Y. M., Amato, G., DeSalle, R., 1999. Captive breeding, reintroduction, and the conservation genetics of black and white ruffed lemurs, *Varecia variegata variegata*. Mol. Ecol. 8, S107-S115.

Xia, X., 2017. DAMBE6: new tools for microbial genomics, phylogenetics, and molecular evolution. J. Hered. 108, 431–437.

Xia, X., Xie, Z., Salemi, M., Chen, L., Wang, Y., 2003. An index of substitution saturation and its application. Mol. Phylogenet. Evol. 26, 1–7.

Yang, C., Xiang, C., Qi, W., Xia, S., Tu, F., Zhang, X., Moermond, T., Yue, B., 2013. Phylogenetic analyses and improved resolution of the family Bovidae based on complete mitochondrial genomes. Biochem. Syst. Ecol. 48, 136–143.

Yule, G. U., 1925. A mathematical theory of evolution, based on the conclusions of Dr. J. C. Willis, F. R. S. Philos. T. Roy. Soc. Lon. B 213, 21–87.

Zhang, D-X., Hewitt, G. M., 1996. Nuclear integrations: challenges for mitochondrial DNA markers. Trends Ecol. Evol. 11, 247-251.

Zhang, D-X., Hewitt, G. M., 2003. Nuclear DNA analyses in genetic studies of populations: practice, problems and prospects. Mol. Ecol. 12, 563–584.

Zimin, A. V., Delcher, A. L., Florea, L., Kelley, D. R., Schatz, M. C., Puiu, D., Hanrahan, F., Pertea, G., Van Tassell, C. P., Sonstegard, T. S., Marçais, G., Roberts, M., Subramanian, P.,

Yorke, J. A., Salzberg, S. L., 2009. A whole-genome assembly of the domestic cow, *Bos taurus*. Genome Biol. 10, R42.

Zink, R. M., 2004. The role of subspecies in obscuring avian biological diversity and misleading conservation policy. Proc. R. Soc. Lond. B. 271, 561-564.

Zink, R. M., Barrowclough, G. F., 2008. Mitochondrial DNA under siege in avian phylogeography. Mol. Ecol. 17, 2107–2121.